



Bearing capacity of pile foundations in Canadian permafrost regions in a
warmer climate

Amro Faki

Department of Civil Engineering
McGill University, Montreal

November 2021

A thesis submitted to McGill University in partial fulfillment of the requirements
of the degree of Master of Engineering.

© Amro Faki 2021

ABSTRACT

The Arctic experienced unprecedented climatic changes in the past few decades and according to the intergovernmental panel on climate change, the warming is projected to continue at twice the rate as for the rest of the world. Adaptation of engineering systems for this region cannot therefore be further delayed. However, one of the major barriers to studies focused on adapting northern engineering systems is the lack of climate change information at the spatial and temporal scales required for engineering applications. This study, to inform decision making, investigates pile bearing capacity for selected pile configurations for the Canadian permafrost regions (Nunavut and Northwest Territories), for current and future climates, using the very first ultra-high resolution (4 km) climate change simulation developed for the region using the Global Environmental Multiscale (GEM) model, for a high emission scenario.

Comparison of the ultra-high-resolution GEM simulation, driven by reanalysis, with available observations confirms the model's ability in representing near-surface permafrost, particularly the continuous extent, and related climate variables. The estimated adfreeze force contribution to the total bearing capacity, for current climate, informed by the reanalysis-driven GEM simulation, for a 5-m cement pile, is found to be of the order of 10% for regions with shallow bedrock and up to 70% for regions with deeper bedrock, within the study domain. Application of the GEM climate change simulation outputs, for RCP8.5 scenario, suggest increases to the active layer thickness, associated with increased ground temperatures, in the 1-3 m range for regions in the southern boundaries of the continuous permafrost extent. Subsequently, decreases to adfreeze force are projected to be in the 5-30% range by 2040, with the largest differences noted for regions with deeper bedrock and warmer permafrost. For steel piles, which are recommended by the Canadian

Standard Association, of same configuration, the projected relative changes will be of similar magnitude, although the adfreeze forces are only about 70% of that for cement piles.

Further downscaling to 250 m resolution using the land model of GEM for the Slave Geological-Grays Bay corridor, where future developments are planned, including an all-season road, enables better estimation of bearing capacity for realistic pile scenarios such as those for bridges (in thick layer of sediments) used for river crossings. Due to the wide variation of pile materials, lengths and installation methods, site specific information can be developed from the framework developed in this study. The results of this study, while providing the first regional-scale analysis for pile bearing capacity over the region, will form the basis for additional detailed investigations on climate-infrastructure interactions and climate resiliency studies.

RÉSUMÉ

L'Arctique a connu des changements climatiques sans précédent au cours des dernières décennies et selon le Groupe d'experts intergouvernemental sur l'évolution du climat (GIEC), le réchauffement devrait se poursuivre à un rythme deux fois plus rapide que pour le reste du monde. L'adaptation des systèmes d'ingénierie pour cette région ne peut pas être davantage retardée. Cependant, l'un des principaux obstacles aux études axées sur l'adaptation des systèmes d'ingénierie nordiques est le manque d'information sur les changements climatiques aux échelles spatiales et temporelles requises pour les applications d'ingénierie. Pour éclairer la prise de décision, cette étude examine la capacité portante des pieux pour des configurations de pieux sélectionnées pour les régions canadiennes de pergélisol (Nunavut et Territoires du Nord-Ouest), pour les climats actuels et futurs, en utilisant la première simulation de changement climatique à ultra-haute résolution (4 km) développée pour la région en utilisant le modèle Global Environmental Multiscale (GEM), pour un scénario d'émissions élevées.

La comparaison de la simulation GEM à ultra-haute résolution, conduite par une réanalyse, avec les observations disponibles confirme la capacité du modèle à représenter le pergélisol proche de la surface, en particulier l'étendue continue, et les variables climatiques associées.

La contribution estimée de l'effort de l'adfreeze à la capacité portante totale, pour le climat actuel, informée par la simulation GEM basée sur la réanalyse, pour un pieu de ciment de 5 m, s'avère être de l'ordre de 10 % pour les régions à substrat rocheux peu profond et jusqu'à 70 % pour les régions à substrat rocheux plus profond dans le domaine d'étude. L'application des résultats de la GEM simulation du changement climatique pour le scénario d'émissions de la voie de concentration représentatives RCP8.5 suggère des augmentations de l'épaisseur de la couche active, associées à une augmentation des températures du sol de l'ordre de 1 à 3 m pour les régions

situées aux limites sud de l'étendue continue du pergélisol. Subséquemment, les diminutions de l'effort de l'adfreeze devraient être de l'ordre de 5 à 30 % à 2040, les plus grandes différences étant notées pour les régions avec un substrat rocheux plus profond et un pergélisol plus chaud. Pour les pieux en acier, qui sont recommandés par l'Association canadienne de normalisation, de même configuration, les changements relatifs projetés seront d'une ampleur similaire, bien que l'effort de l'adfreeze ne représentent qu'environ 70 % de celles des pieux en ciment. Une réduction d'échelle supplémentaire à une résolution de 250 m à l'aide du modèle terrestre de GEM pour le corridor de Slave Geological-Grays Bay, où des développements futurs sont prévus, y compris une route toutes saisons, permet une meilleure estimation de la capacité portante pour des scénarios de pieux réalistes tels que ceux des ponts (dans une épaisse couche de sédiments) utilisés pour les traversées de rivières. En raison de la grande variation des matériaux, des longueurs et des méthodes d'installation des pieux, des informations spécifiques au site peuvent être développées à partir du cadre développé dans cette étude. Les résultats de cette étude, tout en fournissant la première analyse à l'échelle régionale de la capacité portante des pieux dans la région, constitueront la base d'enquêtes détaillées supplémentaires sur les interactions climat-infrastructure et les études de résilience climatique.

ACKNOWLEDGEMENTS

I would like to express my sincere appreciation to my supervisor, Prof. Laxmi Sushama, for her continuous guidance, encouragement, motivation, and support during my master's degree. I would like to thank Prof. Laxmi Sushama for her tremendous efforts in advising me, assistance with the interpretation of the results, and financial support throughout this research. I would like to thank Prof. Guy Doré for his help, guidance, and support throughout the course of this work.

I extend my gratitude to my lab colleagues for the many useful discussions we had, their assistance in preparing and extracting the data, and their valuable advice and incisive comments that made my work much easier.

I would like to thank the Natural Sciences and Engineering Research Council of Canada (NSERC), and Transport Canada for funding this project. I would like to thank Compute Canada/Calcul Québec for providing the computational resources.

I would like to thank my friends for their company, and motivation that helped me overcome the difficulties throughout my studies. Thanks to all the professors and staff members of the department of civil engineering at McGill for their guidance. Finally, I would like to thank my family for their endless support. All of this would not have been possible without their unconditional support and continuous encouragement.

CONTRIBUTION OF AUTHORS

This thesis has been written following the requirements of Graduate and Postdoctoral Studies for a manuscript-based thesis. The main findings of the research undertaken by the author as part of his master's program are presented in a single manuscript. The author carried out the numerical analysis and wrote the manuscript under the supervision of Prof. Laxmi Sushama (supervisor) and Prof. Guy Doré (co-supervisor). The publication detail is presented below:

- Faki, A., Sushama, L., and Doré G. (2021). Regional-scale investigation of pile bearing capacity for Canadian permafrost regions in a warmer climate (To be submitted to 'Cold Regions Science and Technology' journal).

TABLE OF CONTENT

| | |
|---|-----|
| Abstract | I |
| Résumé..... | III |
| Acknowledgements | V |
| Contribution of authors | VI |
| Table of content | VII |
| List of Figures | X |
| List of Tables | XIV |
| CHAPTER 1 - Introduction..... | 1 |
| 1.1 Background | 1 |
| 1.2 Motivation..... | 2 |
| 1.3 Research objectives..... | 3 |
| 1.4 Thesis outline | 4 |
| CHAPTER 2 - Literature Review..... | 5 |
| 2.1 Introduction..... | 5 |
| 2.2 Pile types and installation methods | 6 |
| 2.3 Pile design and bearing capacity estimation | 8 |
| 2.4 Climate change and bearing capacity | 13 |
| 2.4.1 Applicability of climate model outputs in engineering studies | 13 |
| 2.4.2 Studies on bearing capacity and climate change..... | 16 |

| | | |
|---|--|----|
| 2.5 | Climate change adaptation | 18 |
| 2.5.1 | Thermal insulation methods..... | 19 |
| 2.5.2 | Thermosyphons..... | 20 |
| 2.5.3 | Innovation in engineering design..... | 22 |
| 2.6 | Knowledge gaps and conclusions | 24 |
| CHAPTER 3 - Regional scale investigation of pile bearing capacity for Canadian permafrost regions in a warmer climate | | 26 |
| Abstract | | 26 |
| 3.1 | Introduction..... | 28 |
| 3.2 | Model, observed data, and Methods | 31 |
| 3.2.1 | Model and experimental domain | 31 |
| 3.2.2 | Observed data..... | 33 |
| 3.2.3 | Methodology | 34 |
| 3.3 | Model Validation | 37 |
| 3.4 | Projected changes to pile bearing capacity and related climate variables | 41 |
| 3.5 | Slave Geological-Gray's Bay Corridor..... | 44 |
| 3.6 | Summary and conclusions | 49 |
| CHAPTER 4 - Conclusions and Recommendations | | 52 |
| 4.1 | Conclusions..... | 52 |
| 4.2 | Limitations and future research | 53 |

| | |
|------------------|----|
| References | 55 |
|------------------|----|

LIST OF FIGURES

| | |
|---|----|
| Figure 1.1 Forces acting on floating piles embedded in permafrost during summer and winter (for a given scenario); P is the applied load, A.F is the adfreeze force and H.F is the heave force (Andersland and Ladanyi, 1994)..... | 1 |
| Figure 2.1 Observed deterioration of structures. (a) collapsed 5-storey building in Norilsk due to loss of pile bearing capacity. (b) House settlement in Fairbanks. (c) Cracks and deteriorations of building due to permafrost warming. (d) Weathering of foundation caused by intense freeze-thaw cycles. (e) Leakage under the building. (f) Ground subsidence under a kiosk in Norilsk (Edwin and Clarke, 2007; Shiklomanov et al., 2017). | 6 |
| Figure 2.2 Long term cohesion of frozen soils (Weaver and Morgenstern, 1981). | 10 |
| Figure 2.3 Adfreeze bond strength for piles of different materials in different types of soils (Weaver and Morgenstern, 1981). | 11 |
| Figure 2.4 Seasonal mean precipitation (mm/day) for winter (top panels) and summer (bottom panels) obtained from observations (left column) and GEM simulations at 3-km (center column) and 12-km (right column) horizontal resolutions (Diro and Sushama, 2019). | 14 |
| Figure 2.5 Biases in GEM simulations at 50 km (top panels) and 4 km (bottom panels) resolutions with respect to DAYMET for summer average precipitation (%), annual and summer averages of maximum 2-m air temperature (°C) for the 1991-2010 period (Teufel and Sushama, 2021). | 15 |
| Figure 2.6 Reductions in pile bearing capacity by 2050 (Nikiforova and Konnov, 2021). | 17 |
| Figure 2.7 Projected costs of climate change induced damages for the Arctic infrastructure by 2059 (Suter et al., 2019). | 18 |
| Figure 2.8 Example of open ventilated crawl space under heated building (Perreault, 2016) | 19 |

| | |
|---|----|
| Figure 2.9 Passive thermosyphon (Wagner, 2014). | 21 |
| Figure 2.10 Different thermosyphon designs (Wagner, 2014). | 22 |
| Figure 2.11 Grooved pile (a) 3-D diagram and (b) cross-section (Li and Xu, 2007). | 23 |
| Figure 2.12 Different structural versions of self-cooling piles (Plotnikov and Makarov, 2017). | 24 |
| Figure 3.1 (a) Map of Canada showing permafrost extent (four shades of purple from bold to light denote continuous, discontinuous, sporadic, and isolated permafrost, respectively), and observation sites (red, blue, and green asterisks represent ALT, soil boreholes, and MAGT observation sites). (b) GEM experimental domain at 4km (in blue) and 10km (in red) resolutions; gridlines correspond to every 25 th grid point. (c) Depth to bedrock at 4km horizontal resolution (in meters); The black rectangle encloses the Slave Geological-Grays Bay corridor..... | 32 |
| Figure 3.2 (a) Mean daily summer 2m air temperatures (in °C) for Daymet (left panel), and respective biases in GEM4_ERA5 (center panel), and GEM4_CanESM2 (right panel). (b) Mean winter (top row of panels) and spring (bottom row of panels) snow water equivalent (in mm) for CMC and ERA5 reanalysis, and biases in GEM4_ERA5, and GEM4_CanESM2 with respect to CMC..... | 37 |
| Figure 3.3 Observed mean ALT (m) for the 1991-2010 period (stars in the left panel). Also shown are the simulated ALT (for grid points with near-surface permafrost) from GEM4_ERA5 (center panel) and GEM4_CanESM2 (right panel) for the same period. | 38 |
| Figure 3.4 (a) soil temperature at 15-20m depth simulated by GEM4_ERA5 (left panel) and GEM4_CanESM2 (right panel); filled circles represent the observed soil temperature at the depth of zero annual amplitude. (b) Summer and annual soil temperatures at 0.5m depth (left and right panels, respectively); color filled circles indicate GEM4_ERA5 modeled soil temperatures and color filled squares represent the observed soil temperatures. | 39 |

- Figure 3.5** The active layer thickness (ALT, in m; left panels), adfreeze force (in kN; center panels), and total bearing capacity (in kN; right panels) estimated using GEM4_ERA4 (top panels) and GEM4_CanESM2 (bottom panels). 41
- Figure 3.6 (a)** Mean daily summer 2m air temperature (in °C) for the current 1991-2010 period (left panel) and projected changes for the future 2021-2040 period (right panel). **(b)** Mean winter snow water equivalent, in mm, (top panels) and mean spring snow water equivalent (bottom panels) for the current period (left panels) and respective projected changes for the future period (right panels). 42
- Figure 3.7** The estimated ALT (top row) and adfreeze force (bottom row) from GEM4_CanESM2 for the 1991-2010 period (left column) and the respective projected changes for the 2021-2040 period (right column). 43
- Figure 3.8 (a)** Depth to bedrock (m) at 250 m resolution; red asterisks show the location of the points used for the sensitivity analysis presented in Fig. 10 and 11. **(b)** ALT (m), Adfreeze force (kN), and total bearing capacity (kN) at 250-m resolution, over the Slave Geological-Grays Bay Corridor, for the 1991-2010 (top figures) and 2021-2040 (bottom figures) periods. 45
- Figure 3.9** Projected changes to the ALT (m), and adfreeze force (kN) for the Slave Geological-Grays Bay Corridor for the 2021-2040 period respective to 1991-2010 period at 250 m resolution. 46
- Figure 3.10** The 10-year running average of the mean annual temperature (in black) and SWE (in red) obtained from GEM4_CanESM2 with the yearly values shown by a ‘+’ sign. The ALT (m) and adfreeze force (in kN for four different pile scenarios; 5, 10, 15, and 20-m) timeseries for the Northern point. 47

Figure 3.11 The 10-year running average of the mean annual temperature (in black) and SWE (in red) obtained from the GEM4_CanESM2 with the yearly values shown by a '+' sign. The ALT (m) and adfreeze force (in kN for four different pile scenarios; 5, 10, 15, and 20-m) timeseries for the Southern point. 48

LIST OF TABLES

| | |
|--|----|
| Table 2.1 m values for different pile materials (Weaver and Morgenstern, 1981)..... | 10 |
|--|----|

CHAPTER 1 - INTRODUCTION

1.1 Background

In cold regions, shallow foundations, such as tripod footings, are often used for light-weight structures, while piles are used for heavier and settlement sensitive structures. The main function of pile foundations is to transfer loads down to a more stable strata, where possible, or to diminish those loads along the soil column through friction. Pile foundations are favoured in large projects as they can be pre-cast and then installed with less disturbance to the ground's thermal regime, when compared to shallow foundation for which excavation is needed.

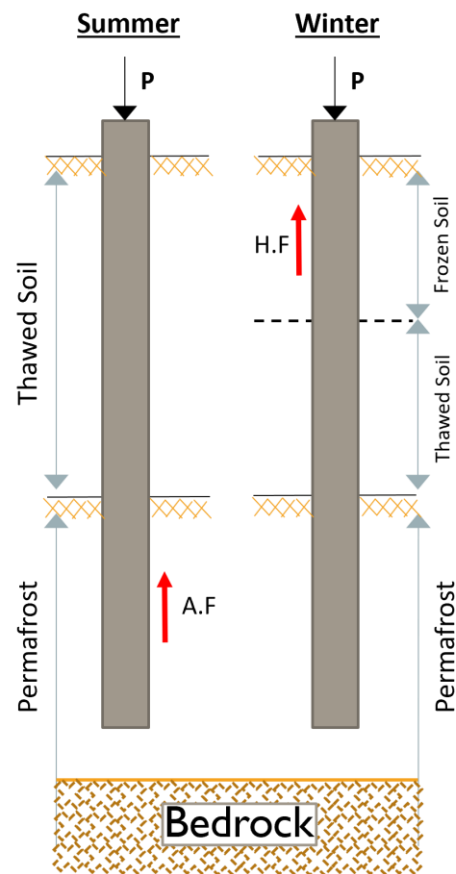


Figure 1.1 Forces acting on floating piles embedded in permafrost during summer and winter (for a given scenario); P is the applied load, $A.F$ is the adfreeze force and $H.F$ is the heave force (Andersland and Ladanyi, 1994).

The stability of pile foundations in permafrost regions, however, can be challenged by many factors, especially in warm seasons, but nonetheless it can be sustained by applying conservative safety factors in the design process. Floating piles in permafrost derive almost all their bearing capacity from what is called the adfreeze force, which is defined as the frictional force generated at the interface between the pile and the surrounding frozen soil. The forces acting on piles in permafrost differ throughout the seasons (Fig. 1.1). In summer, only the portion embedded in permafrost resists the applied loads for floating piles, while in winter, heave forces develop due to the refreezing of near surface soils. Heave force act as an upward-pulling force and need to be considered during the design process. In general, the summer conditions govern the design of piles in frozen grounds (Andersland and Ladanyi, 2003).

1.2 Motivation

Estimating the bearing capacity of pile foundations in frozen ground is crucial for buildings and infrastructure in cold regions, especially now that developments and resource mining are becoming more popular in those regions. Understanding the behaviour of piles embedded in frozen ground whether they rest on a bedrock or frozen soil is critical for the sustainability of newly designed structures and stability of older structures. Furthermore, climate change and associated changes to the active layer thickness and permafrost temperatures can lead to important decrease in bearing capacity. According to the Intergovernmental Panel on Climate Change (IPCC, 2019), 25% of near-surface permafrost (i.e., permafrost in the top 3 to 4m of the soil) is expected to degrade by the end of the century even if global warming is limited to below 2°C; this percentage spikes to 70% if greenhouse gas emissions follow the Representative Concentration Pathway (RCP) 8.5 scenario, which is a high emission scenario. This research, therefore, aims to evaluate projected

changes to pile bearing capacity by mid-century, which can inform climate change adaptation and planning of existing and future infrastructure in the region.

1.3 Research objectives

The main objective of this study is to investigate pile bearing capacity in a warmer climate for the east Canadian Arctic region using the very first convection-permitting transient climate change simulation for the region using the Global Environmental Multiscale (GEM) model for RCP 8.5 emission scenario. More specifically, this study:

- Conducts a literature review on pile foundations in frozen grounds, particularly code recommendations in the Arctic countries, and the applicability and limitations of climate model outputs in informing such engineering-relevant studies;
- Validates the ability of GEM in simulating permafrost and related drivers over Canada using gridded and at-site observations;
- Investigates projected changes to the active layer thickness, permafrost temperature, and consequently, adfreeze force and pile bearing capacity;
- Performs a super-resolution simulation at 250m resolution over the Slave Geological-Grays Bay corridor, which is of transport and resource mining relevance, using the Land Surface Scheme, CLASS, used in GEM, and sensitivity analysis for selected pile configurations to replicate realistic scenarios such as piles in thick sediments as in the case of bridges used for river crossings;
- Draws conclusions on the impacts of climate change on pile bearing capacity which can inform the development of infrastructure in the study region.

1.4 Thesis outline

The thesis herein is divided into four chapters. A general overview discussing the background, motivations, and objectives of this research is presented in the initial sections of Chapter 1. Chapter 2 reviews the existing literature surrounding pile materials, installation methods, and bearing capacity in permafrost regions and on climate modelling tools and their utility in informing adaptation planning, and studies on commonly used adaptation techniques for ground cooling. Chapter 3 is drawn from a journal paper, which presents a regional-scale analysis of pile bearing capacity in Canada's Arctic in a warmer climate. Finally, Chapter 4 presents the summary of the findings and suggestions for future relevant studies. Limitations of this research are also presented in Chapter 4.

CHAPTER 2 - LITERATURE REVIEW

2.1 Introduction

Climate change and associated permafrost degradation can be detrimental to buildings and other infrastructure. In the mid 1960s, a 5-storey building in Norilsk collapsed (Figure 2.1.a) due to the loss of pile bearing capacity (Shiklomanov et al., 2017). Another example of a damaged house in Fairbanks (Figure 2.1.b) is presented by Clarke (2007), where piles were embedded in ice-rich frozen silty soil. Shiklomanov et al. (2017) attributed the prominent permafrost degradation and the consequent instability of infrastructure to four main factors: 1) insufficient consideration of the potential disruption to the thermal state of permafrost caused by the intricate interaction between the different elements of the built structures and frozen ground, Figure 2.1.c is an example of a building that developed structural cracks due to design faults aggravated by permafrost warming; 2) the building quality and the vulnerability to cryogenic weathering of materials (Figure 2.1.d) caused by the harsh Arctic climate that was not considered during the design, which can be elevated by environmental contamination, plus, lack of leakage control and utility maintenance (Figure 2.1.e); 3) the socio-economic conditions that resulted in inadequate developments (Figure 2.1.f; subsidence of a heated kiosk built directly on frozen ground) and lack of necessary actions to prevent snow accumulation, and infrastructure maintenance; 4) climate change and related permafrost degradation. Many previous studies have focused on pile foundations in frozen grounds, including pile materials, installation seasons and methods, methodologies to assess adfreeze bond strength, which are presented below. However, there is a lack of studies focused on climate change impacts on pile bearing capacity, but they are starting to emerge for some regions, which are also reviewed below.

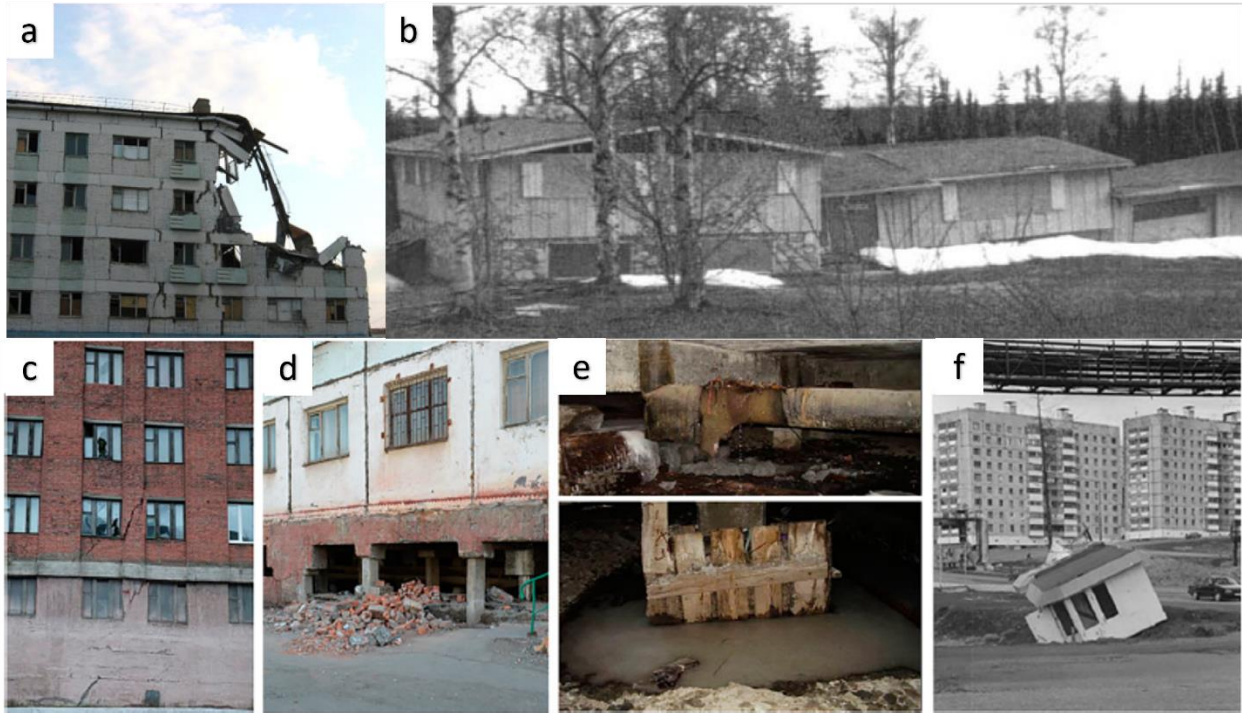


Figure 2.1 Observed deterioration of structures. (a) collapsed 5-storey building in Norilsk due to loss of pile bearing capacity. (b) House settlement in Fairbanks. (c) Cracks and deteriorations of building due to permafrost warming. (d) Weathering of foundation caused by intense freeze-thaw cycles. (e) Leakage under the building. (f) Ground subsidence under a kiosk in Norilsk (Edwin and Clarke, 2007; Shiklomanov et al., 2017).

2.2 Pile types and installation methods

Many types of piles have been used in permafrost, namely, timber, concrete, steel, and composite piles. Various considerations are made in selecting the appropriate pile, such as the type of frozen soil, thermal regime of the permafrost, the expected loads to be transferred, materials and machinery accessibility, and the costs associated with transport and installation (Andersland and Ladanyi, 1994).

Timber piles are usually the most cost-effective solution for some northern communities where timber is available locally. However, it must be noted that it is not always possible to obtain the required lengths and cross sections of timber piles. They remain in good condition in permafrost;

however, care must be taken to prevent decay or deterioration for the part of the pile in the active layer. Timber piles have low thermal conductivity and high adfreeze bond strength; timber shows the highest adfreeze bond strength, followed by concrete and then steel, respectively (Parameswaran, 1978; Parameswaran, 1979). Nonetheless, timber piles are prone to deteriorations exacerbated by rotting, and have limited load carrying capacity which makes them suitable only for light weight structures (Andersland and Ladanyi, 1994; Hoeve and Trimble, 2018). Steel piles can be H-shaped, or pipe-shaped, filled with concrete or sand. According to Andersland and Ladanyi (1994), steel piles do not corrode in permafrost and also show only a small amount of corrosion in the active layer. Steel piles can withstand higher loads than timber piles and is suitable for larger structures. Concrete piles can either be cast-in-place, pre-cast, or pre-cast pre-tensioned. Cast-in-place piles are not very commonly used due to potential disturbance to the ground thermal regime; however, different types of additives have been developed to accelerate the concrete curing process at low temperatures which might make this type of piles workable. Precast and pretensioned concrete piles, although costly to transport due, are widely used in Russia and China and their performance is proved to be sufficient in carrying heavy loads (Li et al., 2016; Yu et al., 2016; Pihlainen, 1959).

Installation methods vary with soil type and temperature and can be briefly summarized as follows: (1) steam thawing of the ground prior to pile driving; (2) hole drilling, using rotary drill or power auger, and pile installation; backfilling is done when the diameter of the hole is larger than the diameter of the pile; (3) direct driving of pile using conventional driving methods, with or without ground temperature modifications. Different combinations of these methods can also be implemented. Helical screw piles are gaining more attention, particularly for use in permafrost regions (Perko, 2009). Helical screw piles are light weight, and have higher bearing capacity and

greater heave force resistance due to the anchor effect of the helices (Fernandez Santoyo et al., 2021). Furthermore, they can be easily installed by applying a torque force at the pile head (Perko, 2009); this favors their use in permafrost regions, where construction time is limited, and transport of larger machinery is challenging.

Different countries have adopted different types of piles based on material availability and costs. In North America, steel pipe piles are commonly used in frozen ground, while in Russia and China, concrete piles are favoured and recommended by the design codes (Shiklomanov et al., 2017; Li et al., 2016; SNIP II-B.6-66, 1966).

2.3 Pile design and bearing capacity estimation

Methods of pile bearing capacity estimation are somewhat similar in North America and Russia with slight differences in the recommended adfreeze bond strengths.

In North America, different methods and recommendations have been adopted throughout the years. Prior to World War II, the construction in Canada's North was limited to small buildings supported on pads or foundations that only extended into shallow depths of permafrost, and due to frost action and thawing of the permafrost, settlements had to be tolerated up to a certain point (Johnston, 1963). Nonetheless, heave forces and the thawing of the active layer necessitated the adoption of new construction methods, especially with northern development. Therefore, foundations that can be embedded in permafrost, such as pile foundations, gained much interest. In 1953, the Canadian government decided to expand its facility in the Northwestern Arctic region, and hence, a plan was put in place to develop the new townsite of Inuvik near the mouth of the Mackenzie River. In 1960, the construction commenced with most buildings designed to be supported on pile foundations. The number of used piles exceeded 20,000 with wooden piles accounting for the largest share since they were locally available. Around 200 cast on site

reinforced concrete piles were selected to carry road bridges, and over 300 were used around corners and along the utilidor lines (Johnston, 1963). Later in 1964, the division of building research of the National Research Council of Canada, NRCC, published a guide for design and construction of pile foundations in permafrost which was translated from the Soviet building code. Following that, in 1976, NRCC translated the Soviet Union standards (SNIP II-B.6-66, 1966) and published it as a handbook for the design of bases and foundations of buildings and other structures on permafrost to be used by professionals then. A pile design procedure was later recommended by Weaver and Morgenstern (1981) recommended a pile design procedure after reviewing the available field test data and published research. They proposed two design procedures based on ultimate bearing capacity and limited settlement. Creep settlement calculations are highly dependent on in-situ conditions; therefore, the ultimate bearing capacity design procedure is discussed here.

The toe resistance of piles embedded in frozen grounds varies greatly with the ice content of the supporting soil. Therefore, a conservative approach is followed when estimating the ultimate bearing capacity of floating piles, in which the tip resistance is disregarded in the calculation, and the bearing capacity is merely estimated from the adfreeze bond strength.

According to Weaver and Morgenstern (1981), when the pile material is very rough, the adfreeze strength is said to be correlated to the long-term shear strength as:

$$\tau_a = m\tau_{lt} \quad (1)$$

where m is related to the pile's surface roughness and typical values are given in Table 2.1 For different materials.

| Pile Type | m |
|-----------------------|-----|
| Steel | 0.6 |
| Concrete | 0.6 |
| Timber (uncreosoted) | 0.7 |
| Corrugated steel pipe | 1.0 |

Table 2.1 m values for different pile materials (Weaver and Morgenstern, 1981).

τ_{lt} is the long-term shear strength of the frozen soil and is related to the friction angle and cohesion of the soil and can be calculated following Mohr-Coulomb equation as:

$$\tau_{lt} = c_{lt} + \sigma \tan \phi_{lt} \quad (2)$$

where c_{lt} and ϕ_{lt} are the cohesive and frictional components, and σ is the normal stress on the adfreeze shear plane. The long-term cohesion of frozen soils can be obtained from Figure 2.2.

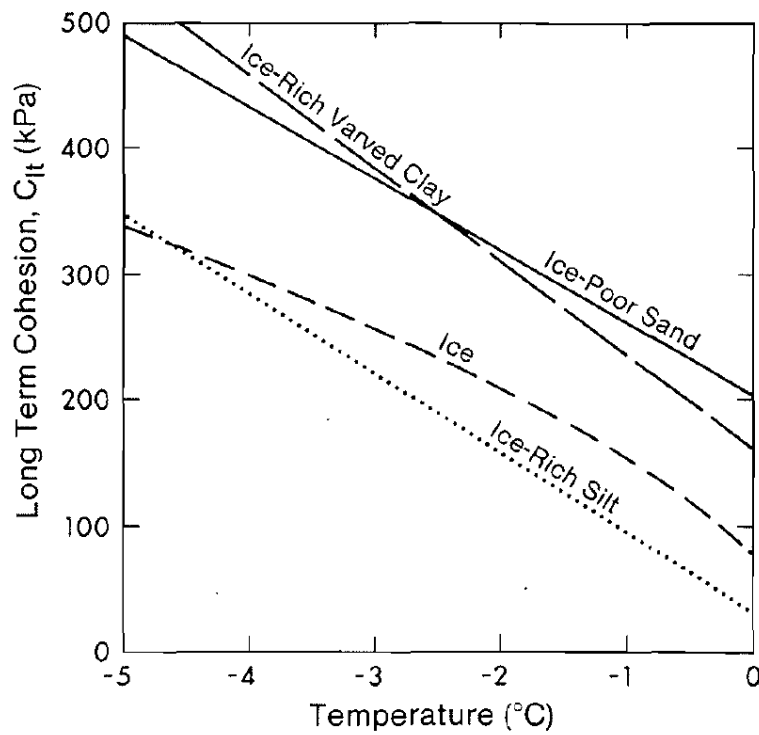


Figure 2.2 Long term cohesion of frozen soils (Weaver and Morgenstern, 1981).

Generally, the frictional part can be neglected, and Eq. (1) reduces to:

$$\tau_a = mc_{lt} \quad (3)$$

The adfreeze strength compiled by Weaver and Morgenstern (1981) from different scientific studies (Crory, 1963; Sanger, 1969; NRCC, 1976) are summarized in Figure 2.3 for different pile materials and soil types.

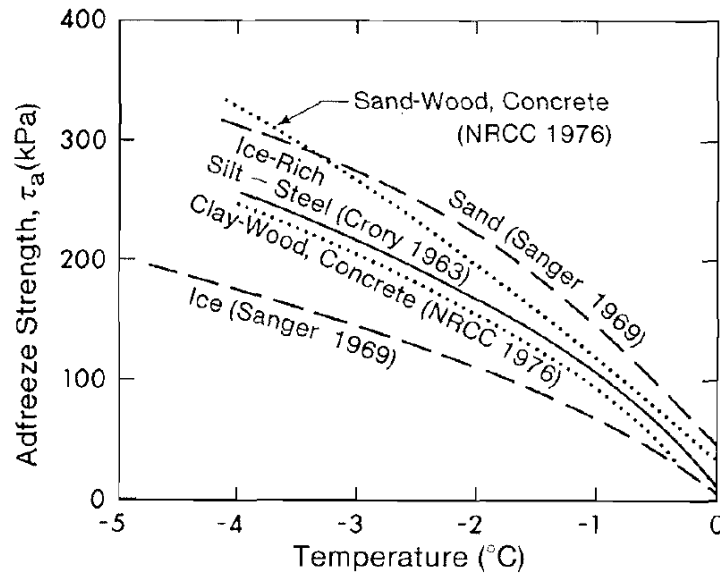


Figure 2.3 Adfreeze bond strength for piles of different materials in different types of soils (Weaver and Morgenstern, 1981).

The above explained methodology seems to be the most trusted procedure to estimate the ultimate bearing capacity in the North American literature. At the present time, this methodology is recommended by the Canadian Standards Association in their document “CSA PLUS 4011.1:19 Technical guide: Design and construction considerations for foundations in permafrost regions”.

The Russian design standards for estimating the bearing capacity in permafrost regions is very similar to that recommended by CSA. Differences are mostly noticed in the suggested adfreeze bond strength values and reduction coefficients for different pile materials. Pile bearing capacity

according to the Russian technical standard; SP 25.13330.2012, soil bases and foundations on permafrost soils, is given as:

$$F_u = \gamma_t \gamma_c (RA + \sum_{i=1}^n R_{af,i} A_{af,i}) \quad (4)$$

Where F_u is in kN, γ_t is the temperature coefficient (mostly equals 1 unless constructing pipelines or a temperature generating structure) and γ_c denotes the working coefficient of the foundation and it is taken as 1 for most cases. R is normal stress at the base of the pile, A is the base area of the pile, $R_{af,i}$ is the adfreeze strength along the shaft of the pile for soil layer i , and $A_{af,i}$ is the area of side contact between the pile and the frozen soil for the same layer. R , and R_{af} values can be obtained from (SP 25.13330.2012) for various soil compositions and ground temperatures. For different pile materials, R_{af} is modified through a multiplication factor, which is provided by the standards. Nonetheless, compared to Weaver and Morgenstern (1981) procedure, the Russian procedure returns lower bearing capacity values, which can be attributed to the more conservative frozen soil cohesion values suggested by the standards. In Morgenstern's procedure, the tables and figures on the adfreeze bond strength are not as well defined as in Russian codes (SP 25.13330.2012). The tables provided by the latter cover a wider range of soil temperatures and compositions; Furthermore, the suggested model recognizes many reduction factors and coefficients to account for different pile materials, methods of installation, potential changes to the ground thermal regime, and the soil ice content.

It is also of importance to mention that in North America, design factors of safety for geotechnical applications are higher than those in Soviet Russia (Streletskiy et al., 2012), which may justify the more conservative values assigned for cohesion in Russian standards.

2.4 Climate change and bearing capacity

2.4.1 Applicability of climate model outputs in engineering studies

Future projections developed using climate models are paramount for studying climate change impacts and assessing vulnerabilities to inform adaptation and mitigation plans. Large-scale climate features (e.g., general circulation of the atmosphere and oceans) can be efficiently simulated by Global Climate Models (Rummukainen, 2010), while regional and local climate variabilities are not captured with the same functionality by the coarse resolution offered by GCMs. This, and the high computational resources required to run high-resolution GCMs, fortified the development of Regional Climate Models, RCMs, by downscaling the climate fields outputted by GCMs to make a transition from large-scale climatic fields to the required smaller-scale fields by dynamical downscaling, i.e., through a limited area physically-based model. RCMs account for the sub-GCM grid scale forcing and physical processes, such as complex topography, coastlines, inland water bodies and land vegetation cover (Giorgi, 2019). GCM outputs are used as the transient boundary conditions to drive RCM simulations; However, biases can be imposed at the lateral boundaries of RCMs. Therefore, to assess the ability of RCMs in simulating the atmospheric fields with reduced systematic biases, a perfect boundary condition experiment can be performed (Rummukainen, 2010; Giorgi, 2019). Such experiments use global reanalysis (e.g., ERA5) to drive the RCM, followed by comparing the simulation outputs with observational datasets to assess the model's performance. Comparison of such a simulation with GCM-driven simulation can help assess the errors associated with the errors in the driving GCM data, i.e., the boundary forcing errors. Model errors and uncertainties in future projections are the most vital challenges to the study of climate modelling. Those errors are especially present in larger grid sizes in both GCMs and RCMs. Furthermore, RCM/GCM resolutions are still considered coarse for many engineering-

scale applications. The above called for an advancement in climate modeling in the form of Convection-Permitting Models, CPMs, which have horizontal resolutions of 4km or smaller. CPMs have made it possible to eliminate the use of convection parameterization schemes which are one of the most vital causes of uncertainties in climate projections (Prein et al., 2015).

In this research, the model used is the limited area version of GEM at convection permitting resolution, i.e., 4-km, with the experimental domain covering Nunavut and the NWT. GEM has been previously used, at different horizontal resolutions, in many studies, and the performance of the model has been established through validation against different observation datasets. Diro and Sushama (2019) investigated the added value of higher resolution simulations by performing two 5-year simulations, using GEM at 3-km (HRES3) and 12-km (MRES12) horizontal resolutions, driven by ERA5 reanalysis at the lateral boundaries.

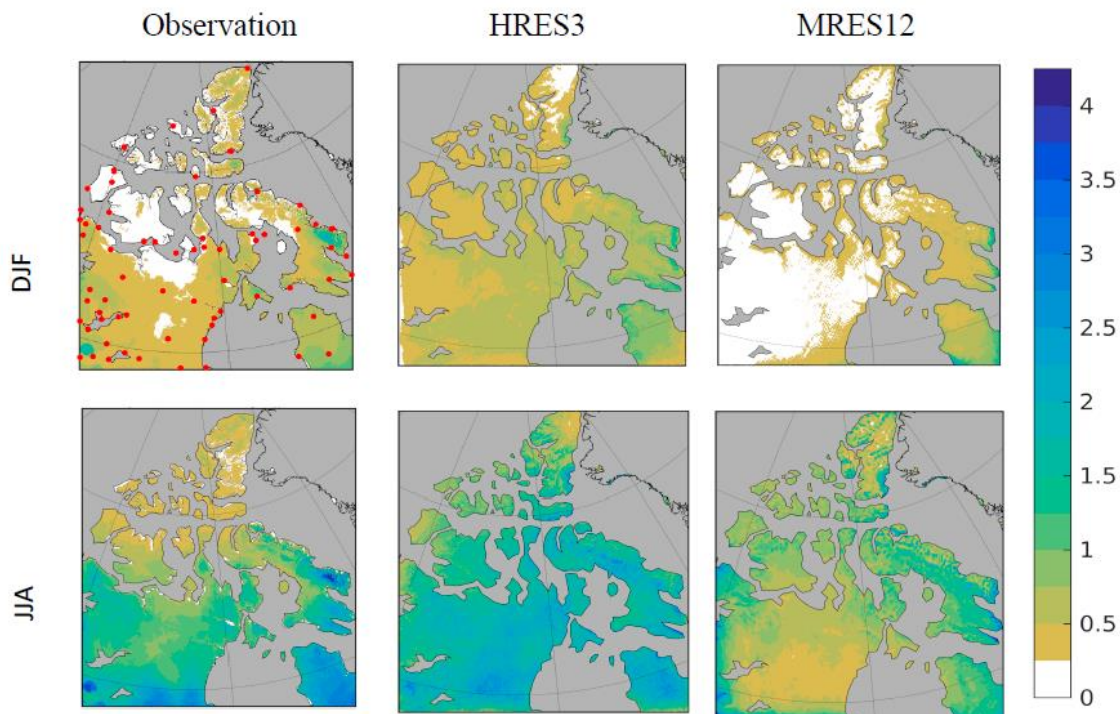


Figure 2.4 Seasonal mean precipitation (mm/day) for winter (top panels) and summer (bottom panels) obtained from observations (left column) and GEM simulations at 3-km (center column) and 12-km (right column) horizontal resolutions (Diro and Sushama, 2019).

Their results show significant improvements in the higher resolution simulation. For instance, as shown in Figure 2.4, the patterns and values of winter and summer mean precipitation (mm/day) are captured more realistically by HRES3 compared to MRES12.

Recently, Tefuel and Sushama (2021) showed the added value of using GEM at convection permitting resolution (4-km). Figure 2.5, from Teufel and Sushama (2021), for example shows biases in the simulated precipitation and temperature fields, from a 4 km and 50 km GEM simulations. Lower biases are observed overall for the 4 km resolution simulation, compared to the 50 km one, highlighting the added value of CPMs.

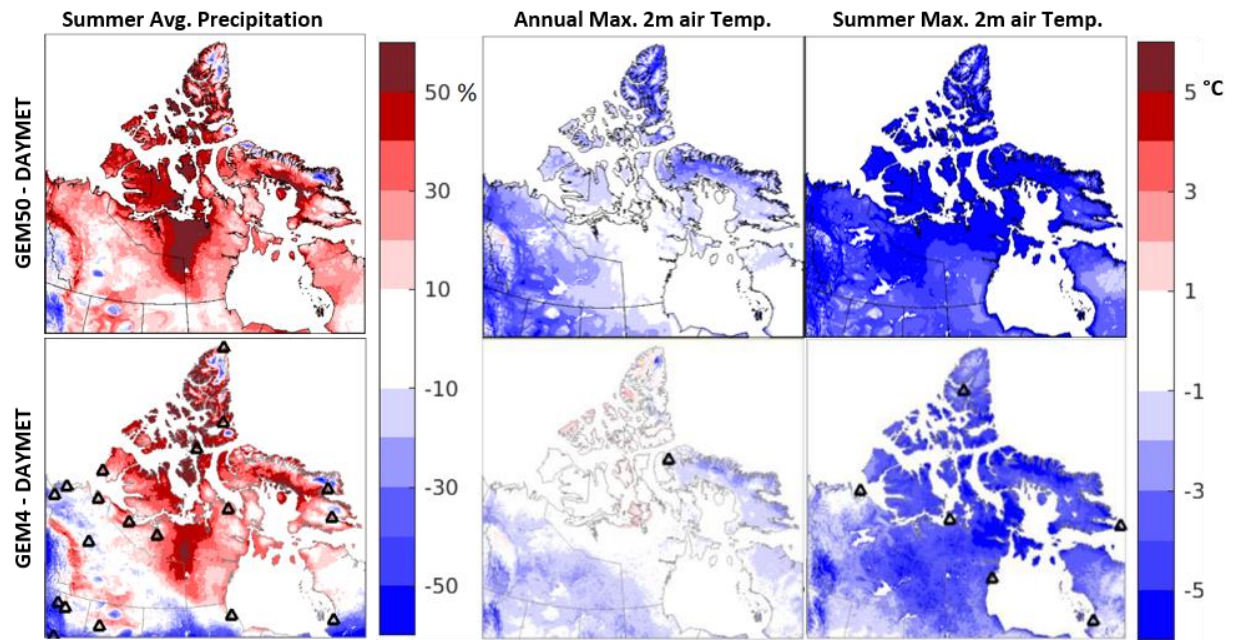


Figure 2.5 Biases in GEM simulations at 50 km (top panels) and 4 km (bottom panels) resolutions with respect to DAYMET for summer average precipitation (%), annual and summer averages of maximum 2-m air temperature (°C) for the 1991-2010 period (Teufel and Sushama, 2021).

2.4.2 Studies on bearing capacity and climate change

Climate modelling has been getting a lot of attention in the geotechnical and infrastructure communities in recent years. When well utilized, climate modelling can be a very important tool to aid professionals and governments in the decision-making process within the framework of climate change adaptation and/or mitigation. Nelson et al. (2001) mapped the expected risks from the degradation of permafrost in the Arctic using the Geophysical Fluid Dynamic Laboratory (GFDL89 scenario) GCM, to categorize permafrost locations into four main zones (i.e., stable, low, moderate, and high-risk zones) depending on hazard potential. Many studies have projected wide degradation to near-surface permafrost using different climate models, resolutions, downscaling methods, and incorporating various risk-based indices (Ran et al., 2018, Teufel and Sushama, 2019, Brooks et al., 2021). More recently, some studies combined climate modelling and geotechnical engineering methods to evaluate potential changes to pile bearing capacity. Streletskiy et al. (2012) estimated changes to the bearing capacity, for a standard 10 m cement pile with a 35x35 cm cross section, induced by climate change in Northwest Siberia and the North Slope of Alaska based on the variation of permafrost temperature and ALT derived from downscaled GCM data. They concluded that the projected climate warming in the Arctic is concerning for infrastructure stability, especially for structures carried on pile foundations that were built using the passive method, where permafrost is protected from thawing during the construction of the structure. In 2012, Streletskiy et al. studied the geographic impact of climate change on infrastructure in the Russian Arctic, and their results indicated a catastrophic decrease of more than 20% to the bearing capacity for a 0.35x0.35x10 m pile, mostly in the southern part of the studied region, associated with increases in the ground temperature and the active layer thickness. Following the same methodology to calculate bearing capacity, Shiklomanov et al.

(2017) used an ensemble of six CMIP5 GCM outputs to assess the stability of infrastructure in the warming Russian Arctic. Their most conservative projections, for the mid-century, indicate less than 25% reduction in the bearing capacity, for a similar 0.35x0.35x10 m cement pile, while the maximum estimates were in the 75-95% range, which would have catastrophic impacts on the region. A similar study by Nikiforova and Konnov (2021) looked at the bearing capacity reduction, for 0.35x0.35x10m piles built with the principle of maintaining the permafrost condition in the 1960s and 1980s, for four geographical regions in the Russian Arctic, results indicate high reductions (>30%) in the bearing capacity of pile foundations over the four regions by 2050 (Fig. 2.6).

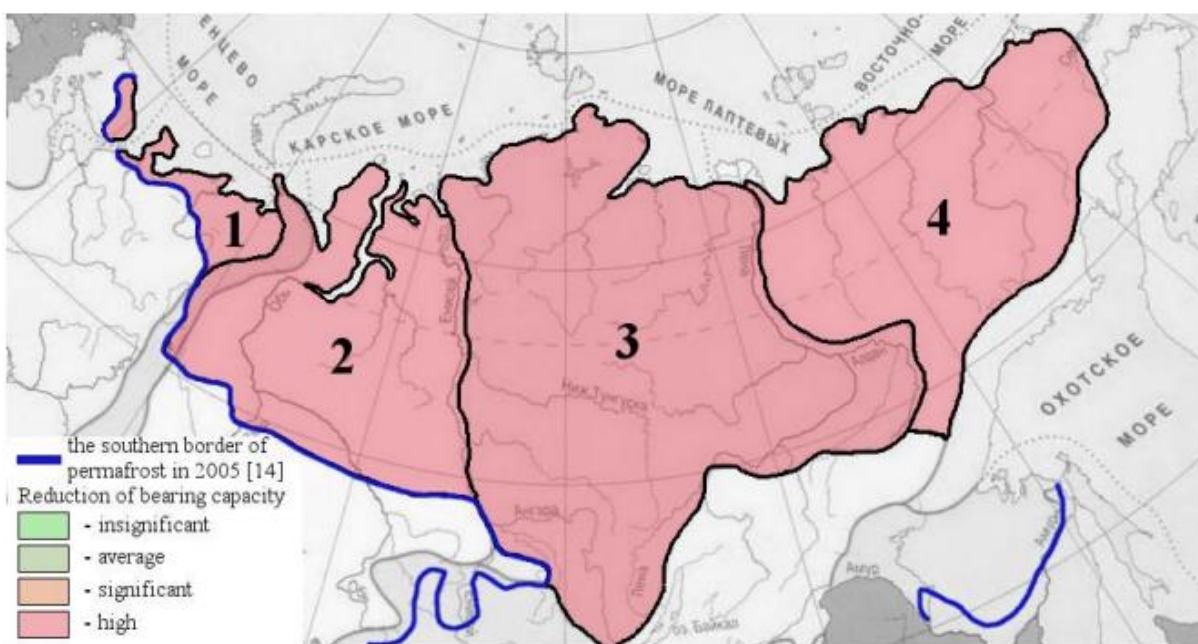


Figure 2.6 Reductions in pile bearing capacity by 2050 (Nikiforova and Konnov, 2021).

Another study by Streletskiy et al. (2019) on the economic impacts of climate change in the Russian permafrost regions, using six CMIP5 models under RCP 8.5 scenario, concluded that changes are projected to distress 54% of residential, 20% of commercial and industrial buildings, and 19% of vital infrastructure facilities with a total sum exceeding 105 billion USD. Suter et al.

(2019) used climate data from six CMIP5 models to estimate changes in permafrost characteristics for RCP8.5 scenario for the Arctic region. The study reported an average reduction of 41% in pile bearing capacity, with a maximum reduction of 69%, for a 0.35x0.35x10m cement pile by 2059. They also constructed a map to show the expected costs of damages, induced by permafrost thawing, to the infrastructure in the Arctic by 2059. Among other regions, Alaska, Yukon, and the Northwest Territories fall under the most impacted regions (Fig 2.7).

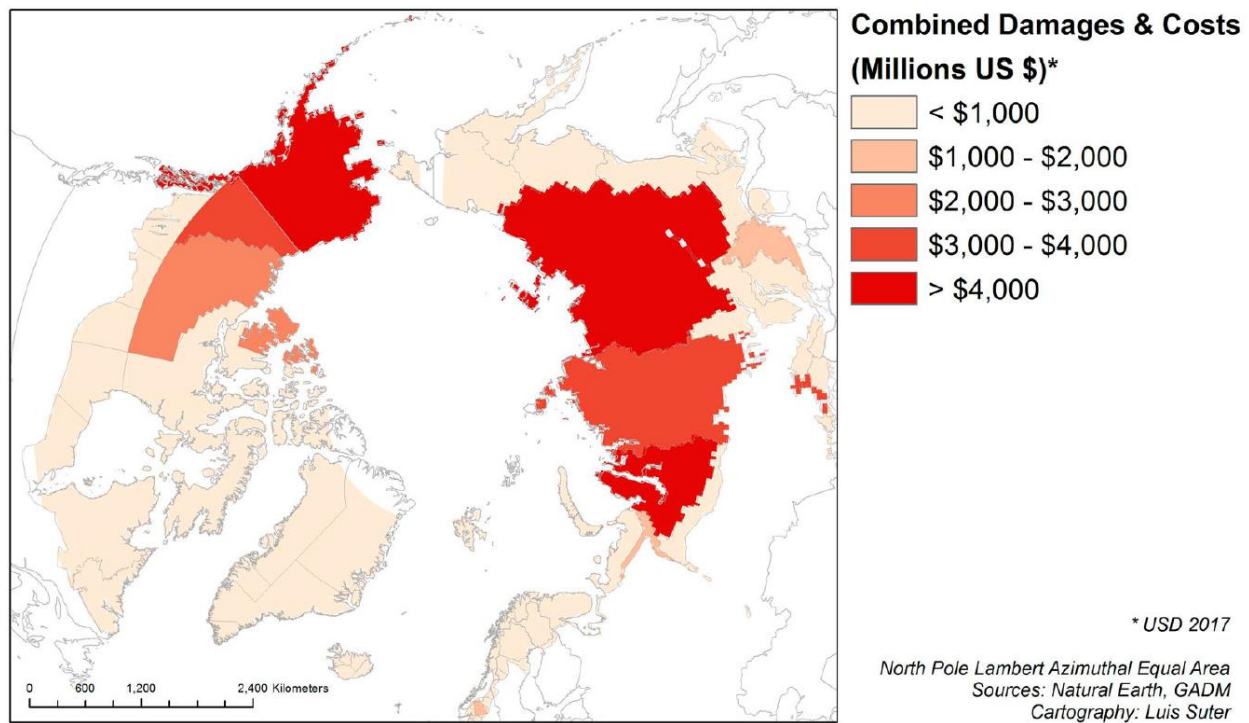


Figure 2.7 Projected costs of climate change induced damages for the Arctic infrastructure by 2059 (Suter et al., 2019).

2.5 Climate change adaptation

As established above, permafrost degradation has been noted for at least half a century and many studies indicate that further warming is inevitable. Therefore, several methods have been and still are being developed and tested to address this issue. There are mainly two types of permafrost protection techniques: one depends on increasing permafrost resistivity to heat exchange

(sometimes referred to as the passive method), and the other is based on directly cooling the frozen ground (e.g., air convection, thermosyphons, ventilation ducts, etc.)

2.5.1 Thermal insulation methods

Thermal insulation is attained by limiting the heat transfer to the permafrost table through increasing the thermal resistance of the interface between the permafrost and the upper surface (Cheng et al., 2004). Many procedures, for the purpose of increasing the interface's thermal resistance, have been reported in the literature. A very common practice when building on frozen ground is to elevate the structure above the ground creating what is called an open ventilated crawl space (Fig. 2.8), the space allows for air circulation below the structure which helps with the soil cooling process (Shur and Goering, 2009).



Figure 2.8 Example of open ventilated crawl space under heated building (Perreault, 2016)

Another method that was used to stabilize the ground around pile foundations was reported in Miller and Johnson (2000). A problem of creep settlement was encountered, and the proposed solution was to cover the ground surface under the crawl space with a smooth thin sand layer followed by two 50-mm thick layers of insulation and a protective membrane was used as well. Close site monitoring deemed the solution a success. However, further studies pointed out a downside for such insulation method. For instance, Perreault and Shur (2016) analyzed the impact

of permanent versus seasonal insulation on the ground's thermal regime. Permanent insulation can effectively reduce the thawing of permafrost under heated structures (e.g., residential buildings, warm pipelines). Peatlands represent a natural permanent layer of insulation in which the thermal properties are seasonally altered. Although some studies agree with the previous statement (Porkhaev, 1970; Farouki, 1992; Shur et al., 2004), many field observations do not support the same conclusion. Pavlov (1975) concluded that permanent insulation below unheated structures have a warming effect on the permafrost in regions where the mean annual air temperature is under 0°C , and a cooling effect where the mean annual air temperature exceeds 0°C . On the other hand, seasonal thermal insulation, in Summer, was found to be more effective in decreasing frozen ground temperatures and lessen the active layer thickness leading to a controlled frost heave forces on the foundation (snow is an example of a natural seasonal insulation). The impact was found to be greater for higher thawing index values (Perreault and Shur, 2016). Such seasonal insulation is believed to be most valuable in the discontinuous permafrost region, where minor ground temperature changes can have a major impact on the bearing capacity and adfreeze force. Nonetheless, thermal insulation alone will not be enough to stabilize the ground with the warming climate (Cheng et al., 2004), therefore, other mitigation techniques need to be utilized.

2.5.2 Thermosyphons

A thermal pile is a pile that transfers heat from the ground to the air by natural convection or if it is designed to have a cooling system based on forced circulations (Johnston, 1981).

Thermosyphons are conventionally made from a two-phase system, which include an underground (buried) evaporation system and an above ground (air-exposed) condensation system (Fig 2.9).

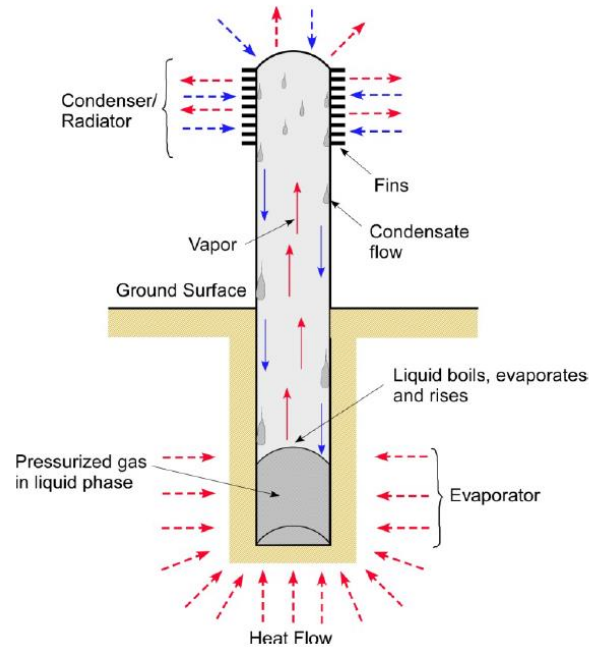


Figure 2.9 Passive thermosyphon (Wagner, 2014).

The pipe works with the thermal convection principle, it is loaded with a single compound working fluid that evaporates at the base of the pipe when absorbing temperature from the soil, then the light density vapor moves up to the condenser where it is cooled and liquidized again and then the condensed liquid returns to the evaporation part by the force of gravity creating a one-way heat transport from the warmer ground to the cooler air. The concept of heat circulation found its way to structure stabilization in frozen ground in many different ways (Holubec, 2008).

Thermosyphons have been developed to take many forms (Fig. 2.10) in order to accommodate the different requirements of different structures (Wagner, 2014); a) Thermoprobes are vertical non-structural pipes usually installed around piles or different structures to extract the heat from the soil and keep the ground frozen. Thermoprobes are the first application of Thermosyphons. b) Sloped-Thermosyphon-Foundations where the buried part is sloped below the building foundation to cover a wider cooling area. c) Flat-Thermosyphons where the evaporator is laid to be absolutely horizontal under the foundation to ensure a uniform distribution of the working fluid and uniform

heat extraction, subsequently. d) Flat-Loop-Thermosyphon-Foundations, with the buried part laid flat below the foundation covering 1.4 times the volume of frozen soil in comparison to type (b). e) Hairpin-Thermosyphons where both the condenser and the evaporator are buried, providing a solution for roads and runways. Furthermore, a hybrid Flat-Loop-Thermosyphon was later developed by introducing a mechanical cooler to the system to improve the rate of soil cooling; the cooler is triggered when the air temperature is not cold enough to condense the working fluid.

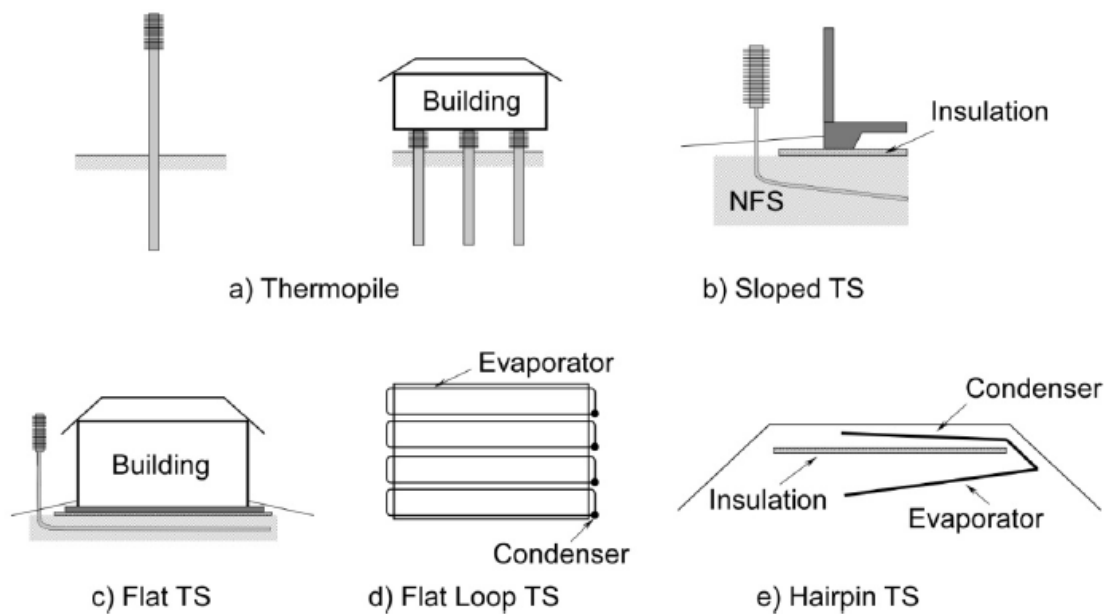


Figure 2.10 Different thermosyphon designs (Wagner, 2014).

2.5.3 Innovation in engineering design

This section discusses some of the pioneering work on pile design for the purpose of permafrost cooling and preservation.

Li and Xu (2007) proposed a new pile design for dry bridges and ventilated foundations. The pile is designed to be grooved in the active layer section of the soil and then filled with a porous material (Fig 2.11).

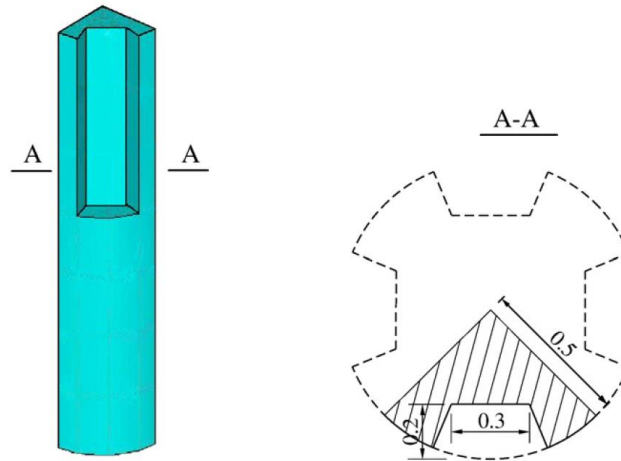


Figure 2.11 Grooved pile (a) 3-D diagram and (b) cross-section (Li and Xu, 2007).

In winter, the lower-density warm air in the bottom part of the grooves moves upwards due to buoyancy-driven convection, and colder air moves downwards cooling the surrounding soil, while in summer the lower density air is present above the ground surface which prevents any convection. Results for cast-in-place and pre-cast grooved piles show an increase in the bearing capacity of 16% and 21%, respectively, while the heave forces are shown to be reduced by 80%. Many attempts at pile designs and soil cooling methods have been reported in the literature. However, so far, the greatest innovation related to ground cooling in permafrost regions is Thermopiles or Cold piles (Zarling and Yarmak, 2007; Plotnikov and Makarov, 2017), which comprises of a thermosyphon embedded into a conventional pile. Figure 2.12 shows different versions of self-cooling piles. The used thermosyphons can be evaporative or liquid-type, the main difference between the two types is the rate of heat exchange, where the evaporative type is shown to have 10-30 times more higher heat exchange coefficient. Evaporative-type piles are more efficient when it comes to freezing thawed grounds, while liquid-type piles are beneficial in cooling frozen ground (Plotnikov and Makarov, 2017).

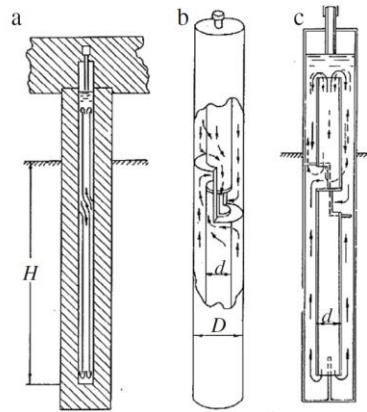


Figure 2.12 Different structural versions of self-cooling piles (Plotnikov and Makarov, 2017).

Furthermore, Huang et al. (2019) proposed the idea of a self-operating helical energy pile that they referred to as Thermo-syphon Helical Pile (THP). Their structural stability analysis and feasibility study deemed the pile a promising alternative to energy piles in frozen ground for both new and retrofitted buildings.

2.6 Knowledge gaps and conclusions

The study of the integrity of buildings and other infrastructures in permafrost regions in relation to climate warming is a growing field of research, given the need to adapt to a changing climate and mitigate the drastic potential consequences. Very few studies have focussed on the impacts of climate change on the geotechnical stability of infrastructure, especially for Canadian permafrost regions. Another cause for concern is the lack of published observation data and site measurements with the required spatial coverage, particularly for Canada, which would be useful in validating climate models and enhance any subsequent engineering-relevant analysis. Besides that, there is a lack of detailed climate projections, for Canada's northern regions, that are needed for informing engineering adaptation studies, such as pile bearing capacity estimations in a changing climate.

This thesis addresses this knowledge gap by developing detailed climate change information using the limited version of global environment multiscale (GEM) model which has been applied and

validated broadly in climate related studies (Jeong and Sushama, 2019; Teufel and Sushama., 2019; Oh and Sushama, 2020; Zhao and Sushama, 2020; Dukhan and Sushama, 2021).

Based on literature review, it was decided to use the pile bearing capacity estimation method suggested by the Russian design standards in this study. The methods suggested by the standards were previously used in several studies (Streletskiy et al., 2012; Shiklomanov et al., 2017). In this study, the pile bearing capacity estimation is informed by ultra-high-resolution climate simulation outputs performed over Canada's Arctic region (detailed descriptions of the used models are presented in Chapter 3 along with the results).

CHAPTER 3 - REGIONAL SCALE INVESTIGATION OF PILE BEARING CAPACITY FOR CANADIAN PERMAFROST REGIONS IN A WARMER CLIMATE

Amro Faki*, Laxmi Sushama¹, Guy Doré²

¹ Department of Civil Engineering, Trottier Institute for Sustainability in Engineering and Design, McGill University, Montreal, QC, Canada

² Department of Civil Engineering and Water Engineering, Laval University, QC, Canada

*Corresponding author E-mail: amro.faki@mail.mcgill.ca

ABSTRACT

Climate change is being experienced particularly intensely in the Arctic and therefore adaptation of engineering systems for this region cannot be further delayed. However, one of the major barriers to studies focused on adapting northern engineering systems is the lack of information at the spatial and temporal scales required for engineering applications. This study investigates pile bearing capacity for selected pile configurations for the Canadian permafrost regions (Nunavut and Northwest Territories), for current and future climates, using the very first ultra-high resolution (4 km) climate change simulation developed for the region using the Global Environmental Multiscale (GEM) model, for a high emission scenario.

Comparison of the ultra-high-resolution GEM simulation, driven by reanalysis, with available observations confirms the model's ability in representing near-surface permafrost and related climate variables. The estimated adfreeze contribution to the total bearing capacity, for current climate, informed by the reanalysis-driven GEM simulation, for a 5-m cement pile, is found to be of the order of 15% for regions with shallow bedrock and 80% for regions with deeper bedrock. Application of the GEM climate change simulation outputs, for RCP8.5 scenario, suggest

decreases to adfreeze contribution in the 5-30% range by 2040, with the largest differences noted for regions with deeper bedrock. For steel piles of same configuration, although the adfreeze contributions are only about 70% of that for cement piles, the projected relative changes are of similar magnitude.

Further downscaling to 250 m resolution using the land model of GEM for the Slave Geological-Grays Bay corridor, where future developments are planned, including an all-season road, enables better estimation of bearing capacity for realistic pile scenarios such as those for bridges (in thick layer of sediments) used for river crossings. Due to the wide variation of pile materials, lengths and installation methods, site specific information can be developed from the framework developed in this study. The results of this study, including the ultra-high resolution climate change information, will thus form the basis for additional detailed investigations on climate-infrastructure interactions and climate resiliency studies.

Keywords: Climate change, permafrost, convection-permitting resolution, pile foundation, bearing capacity, adfreeze force, active layer.

3.1 Introduction

According to the sixth assessment report of the intergovernmental panel on climate change (IPCC, 2021), the Arctic region will continue to warm at double the rate of the global mean. Arctic amplification is primarily responsible for this intensified warming, and is attributable to several factors, such as snow and sea ice cover loss which leads to reduced summer albedo, the total water vapor increase in the atmosphere, changes in summer cloud cover, heat generated by the lately formed sea ice across major open water areas in autumn, northerly conveyance of heat and moisture, and the lower level of heat loss to the outer space from the Arctic compared to the equatorial regions (Goosse et al., 2018; Pithan and Mauritsen, 2014; Serreze and Barry, 2011; Stuecker et al., 2018; IPCC, 2019). About 50% of Canada is underlain by permafrost, which is defined as soil or rock that remains frozen for at least two consecutive years. According to the recent special report on the ocean and cryosphere in a changing climate (IPCC, 2019), even if global warming is limited to below 2°C, 25% of near-surface permafrost, i.e., permafrost in the top 3 to 4 m, is estimated to degrade by the end of the century, while 70% of near-surface permafrost is expected to degrade if greenhouse gas emissions follow the Representative Concentration Pathway (RCP) 8.5 scenario. This degradation of permafrost is a key concern for infrastructure stability in these regions (Shiklomanov et al., 2017; Streletskiy et al., 2012), particularly for the southern limit of the permafrost zone (Liu et al., 2020).

The common practice when building in permafrost regions is to elevate heated structures (e.g., pipelines, residential and commercial buildings) above the ground surface to facilitate air circulation below the structure, thus contributing to soil cooling, and eliminating any heat exchange that would induce permafrost thaw (Andersland and Ladanyi, 2003). To achieve the above, several forms of substructures have been adopted. For instance, in Russia, 75% of buildings

are found on pile foundations (Shiklomanov et al., 2017). In Norway, pile foundations are the most used type of foundation, while in Northern Canada, the most used foundation for buildings is tripod footing which was adopted due to its lower initial cost and ease of construction (Harries, 2018). Nevertheless, many issues are associated with the use of tripod footing with differential settlements being the most important concern, which could be exacerbated in a warmer climate and therefore, according to Harries (2018), pile foundations would be a better strategy to support buildings on permafrost.

Wooden, concrete, and steel piles have been successfully used in cold regions. In North America, steel pipe piles are favored due to their availability, ease of transport, practicality of installation, and workability (Couture et al., 2000; Sanger, 1969), while in Russia, concrete piles are dominantly used for traditional construction (Streletskiy et al., 2012). However, although concrete piles show higher adfreeze forces and better behavior in resisting frost heave (Parameswaran, 1978, 1979), they come with their own challenges; when piles are cast-in-place, arrangements must be made to address the vulnerability of permafrost to thaw due to the heat generated by cement hydration (Gao et al., 2019). Cast-on-site piles also require special attention to regulate the concrete setting time, and control shrinkage cracks (Korhonen and Brook, 1996). As for precast piles, their use is limited in permafrost regions due to the high costs associated with their transport and the need for skilled labor (Dennison, 2017; Pihlainen, 1959).

Irrespective of the type of pile foundation used, it is important to consider climate change impacts on the bearing capacity, especially for floating piles. Streletskiy et al. (2012) studied climate change impacts on pile bearing capacity, for a 0.35x0.35x10-m cement pile, for the North Slope of Alaska, using a statistically downscaled output (at 2-km horizontal resolution) from five phase-5 Coupled Model Intercomparison Project (CMIP5) Global Climate Models (GCMs) for RCP6.0

scenario. Their results suggest decreases of up to 80% in pile bearing capacity for their study region by 2040. Shiklomanov et al. (2017) evaluated the stability of urban infrastructure in the Russian Arctic using an ensemble of six CMIP5 GCM simulations rescaled to 100-km horizontal resolution and reported critical decreases of up to 75% in pile bearing capacity, for RCP8.5 emission scenario, that can destabilize structures by 2050.

Adaptation of engineering and infrastructure systems to possible warming scenarios is limited by the lack of actionable climate information, i.e., climate change information at engineering scales. Though regional climate models (RCMs) can be used for downscaling GCMs dynamically, they are still available at 10 to 20 km resolution, which is insufficient to describe many important processes that rarely extend beyond a few kilometers (e.g., convective cloud systems). A promising approach is the use of ultra-high resolution convection-permitting models (CPMs), with horizontal resolutions of 4 km and finer. Besides explicitly resolving deep convection, CPMs also offer the advantage of further improving the representation of fine-scale orography and surface heterogeneity when compared to RCMs (Prein et al., 2013a, 2013b). Limited-area modelling is the approach most frequently used for CPM climate simulations. This approach telescopically nests limited-area domains at increasing horizontal resolution until convection-permitting scales are reached (e.g., Prein et al., 2013b). CPM climate simulations are able to provide information at the spatial and temporal scales required for many engineering applications.

Therefore, the main purpose of this study is to investigate the pile bearing capacity for the Eastern Canadian permafrost region, using the very first ultra-high resolution, i.e., 4-km, climate change simulation performed over the region. The study also presents detailed offline land surface modelling at 250 m resolution over the Slave Geological-Grays Bay Corridor, which is of interest from future infrastructure and resource mining development perspectives.

This paper is organized into 5 main sections, including the introduction. Section 3.2 gives details of the climate model, simulations, observation datasets used for validation, and the methodology used to estimate pile bearing capacity. Section 3.3 discusses climate model validation results and bearing capacity estimates for current climate, and projected changes to pile bearing capacity and related climate variables are presented in section 3.4. Section 3.5 gives detailed analysis of pile bearing capacity for the corridor of interest and selected sensitivity experiments. Summary and conclusions are provided in section 3.6.

3.2 Model, observed data, and Methods

3.2.1 Model and experimental domain

In this study, the limited area version of the Global Environmental Multiscale (GEM) model (Côté et al., 1998) that uses a non-hydrostatic dynamical core with a hybrid vertical coordinate is used to perform convection-permitting climate simulations. More details about the model can be found in Diro and Sushama (2019), but a brief description of the physics parameterization is given here. Besides the large-scale precipitation schemes, convective processes are represented in the model following Kain and Fritsch (1990) for deep convection and Bélair et al. (2005) for shallow convection. The resolvable large-scale precipitation is computed following Sundqvist et al. (1989). Radiation is parametrized by Correlated K solar and terrestrial radiation of (Li and Barker, 2005). The planetary boundary layer scheme follows Benoit et al. (1989) and Delage (1997), with some modifications as described in Zadra et al. (2012). Lakes, both resolved and sub-grid scale, are represented by the Flake model (Martynov et al., 2010; Mironov et al., 2005). The land surface scheme used in GEM is the Canadian Land Surface Scheme (CLASS) (Verseghy, 2009), which allows flexible soil layer configuration. A 60 m deep land surface configuration with 26 layers is used in the GEM simulations, which is particularly important for interactive modelling of

permafrost. The layer thicknesses in m, starting from the surface down, are as follows: 0.1, 0.2, 0.3, 0.4, 0.5 (10 layers), 1.0, 3.0, and 5.0 (10 layers).

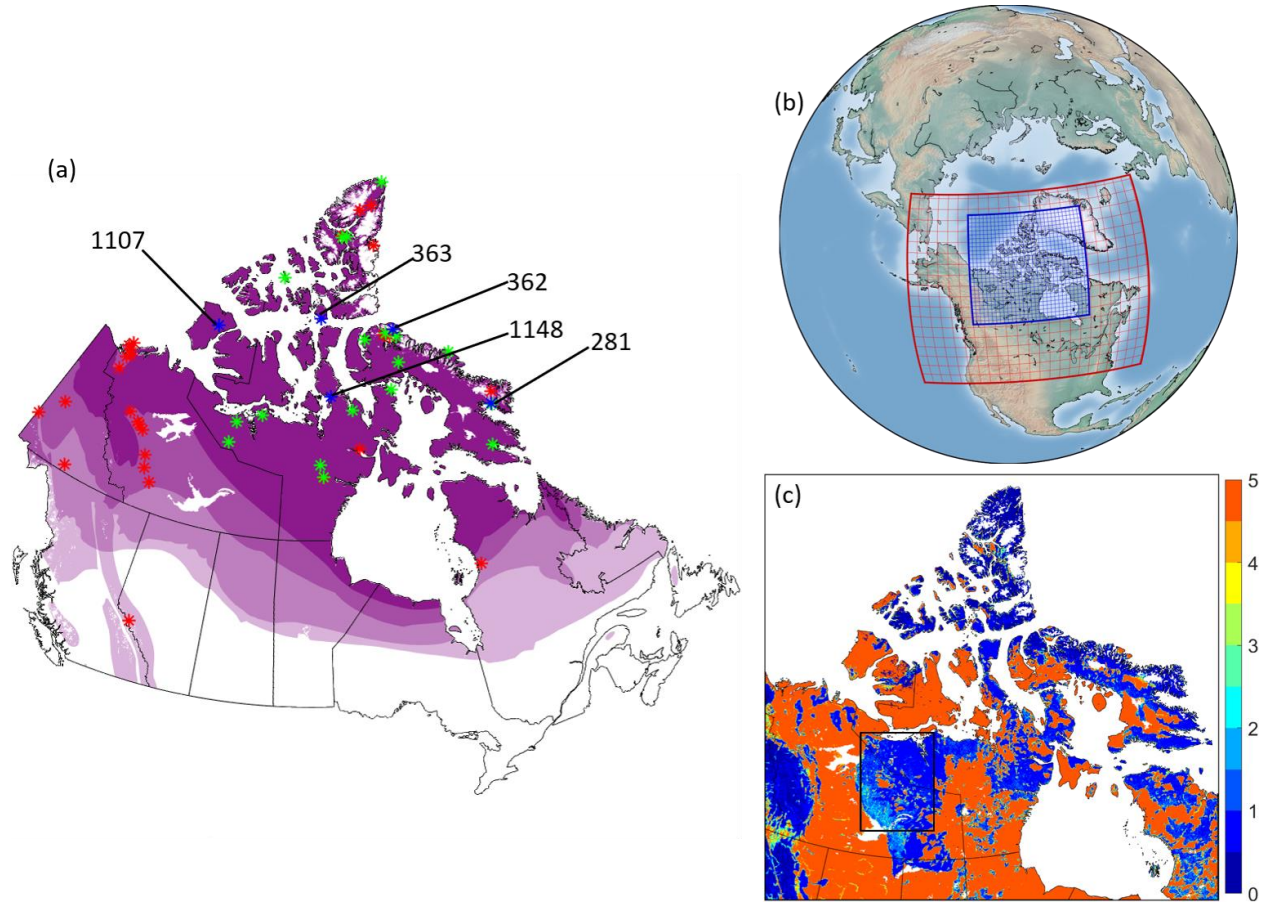


Figure 3.1 (a) Map of Canada showing permafrost extent (four shades of purple from bold to light denote continuous, discontinuous, sporadic, and isolated permafrost, respectively), and observation sites (red, blue, and green asterisks represent ALT, soil boreholes, and MAGT observation sites). (b) GEM experimental domain at 4km (in blue) and 10km (in red) resolutions; gridlines correspond to every 25th grid point. (c) Depth to bedrock at 4km horizontal resolution (in meters); The black rectangle encloses the Slave Geological-Grays Bay corridor.

For this study, two simulations are performed using GEM. The first one, a validation simulation, is driven by ERA5 reanalysis (Hersbach et al., 2020) for the 1991-2010 period, over the interior 4 km resolution domain shown in Fig. 3.1b, comprising of 748x700 grid points covering Nunavut and the Northwest territories. This simulation will be referred to as GEM4_ERA5. The second one is a transient climate change simulation, spanning the 1989-2040 period, and downscales a single member of an initial condition ensemble of the Second-Generation Canadian Earth System Model

(CanESM2) for the RCP8.5 scenario, using a grid-telescoping approach; the RCP8.5 scenario corresponds to the highest greenhouse gas emissions scenario and does not include any specific climate mitigation target, leading to a radiative forcing of 8.5 W/m^2 at the end of 21st century (Riahi et al., 2011). CanESM2 is initially downscaled to a 10km resolution pan-Canadian grid consisting of 580x460 grid points (GEM10_CanESM2), which is then used as the lateral boundary conditions for the ultra-high convection-permitting resolution simulation over the inner 4 km domain. Although this 4 km simulation is driven by the outputs of GEM10_CanESM2, it will be referred to as GEM4_CanESM2 for easy distinction with the 4 km resolution ERA5-driven simulation.

Furthermore, since surface heterogeneity is hard to capture even at 4 km resolution, offline simulations with the land component of GEM, CLASS, driven by GEM4_CanESM2 outputs (air temperature, precipitation, radiative fluxes at the surface, surface air pressure, specific humidity, wind velocity), at 250 m resolution, are performed over the Slave Geological-Gray's Bay Corridor. This is a region where future developments are planned, including the construction of an all-season road. To better capture the near-surface ground thermal and moisture regimes, the 60-m deep CLASS in the offline simulations is configured to have 72 layers with the following thicknesses in m (from the surface downwards): 0.1, 0.2 (32 layers), 0.3 (5 layers), 0.4 (5 layers), 0.5 (10 layers), 1.0 (10 layers), 3.0 (5 layers), 5.0 (4 layers).

3.2.2 Observed data

For model validation, 2m air temperature from Daymet (Thornton et al., 2016), which is available at 1 km horizontal resolution, is used. Snow water equivalent (SWE) from the Canadian Metrological Centre, CMC, at 24 km resolution (Brown and Brasnett, 2010), and ERA5 reanalysis (Hersbach et al., 2020), at 30 km horizontal resolution, are used for snow validation. Model

simulated soil temperatures are validated against those from the Global Terrestrial Network for Permafrost (GTN-P, 2015). Additionally, soil temperature measurements near the depth of zero annual amplitude (also referred to as the mean annual ground temperature, MAGT) at 20 locations from the Geological Survey of Canada (Smith et al., 2013) are also used for model validation. As for the active layer thickness validation, the Circumpolar Active Layer Monitoring Network (CALM) data for 35 locations are used (Brown et al., 2000). Additional data from 9 ALT monitoring sites in the Mackenzie valley corridor (Duchesne et al., 2018) are also used. The locations of the MAGT, soil temperature, and ALT observation sites are shown in Fig. 3.1a.

3.2.3 Methodology

The first step prior to using GEM simulation outputs in estimating pile bearing capacity is to test the ability of the model in simulating relevant climate variables by comparing GEM4_ERA5 with observations. The same GEM simulations considered in this study were used in Teufel and Sushama (2021), where a thorough validation of the model is presented. Nonetheless, since the focus of this study is on pile bearing capacity, which changes with evolving active layer thickness (ALT), the main climate variables that influence ALT, namely 2-m summer air temperature, spring (MAM) and winter (DJF) snow water equivalent (SWE), are validated by comparing with datasets discussed in Section 3.2.2. Model simulated soil temperatures at 0.5-m depth, MAGT, and ALT are also validated against site observations (sources discussed in section 3.2.2). Furthermore, comparison of GEM4_CanESM2 with GEM4_ERA5 is undertaken to identify regions with large differences, which is due to errors in the downscaled CanESM2 driving data, where extra caution is required when interpreting projected changes.

In this study, the bearing capacity of pile foundations, F_u , is estimated, for a 5m cement pile with a square cross-section of 0.35mx0.35m, following the method suggested by the Russian Federation standards for soil basis and foundations on permafrost soils (SP 25.13330.2012, 2012) as:

$$F_u = \gamma_t \gamma_c (RA + \sum_{i=1}^n R_{af,i} A_{af,i}), \quad (1)$$

F_u (in kN) is therefore the sum of the normal stress acting at the bottom of the pile and shear stress on the sides of the pile that come in contact with the frozen soil (also known as the adfreeze strength), represented by the first and second terms on the right hand side of Eq. (1), respectively; γ_t is the temperature coefficient (equals 1, except for pipelines and temperature generating structures) and γ_c denotes the working coefficient of the foundation and it is taken as 1 for most cases; R is normal stress at the base of the pile, A is the base area of the pile, $R_{af,i}$ is the adfreeze strength along the shaft of the pile for soil layer i , and $A_{af,i}$ is the area of side contact between the pile and the frozen soil for the layer. R_{af} values can be obtained from SP 25.13330.2012 (2012) for various soil compositions and ground temperatures. Reduction factors/coefficients can be applied to Eq. (1) to account for different methods of installation and pile materials. For example, for steel piles, a factor of 0.7 should be applied to R_{af} , which will yield adfreeze forces that are reduced by 30%, when compared to those for cement piles. The toe resistance of piles embedded in frozen grounds is highly contingent on the salinity and ice content of the supporting soil. Therefore, the tip resistance is ignored, following a conservative approach, in the ultimate bearing capacity calculations for a floating pile and the adfreeze bond strength is considered to be the sole contributor.

The pile bearing capacity estimation proposed by the Canadian Standards Association's technical guide CSA PLUS 4011.1:19, which follows Weaver and Morgenstern (1981), is similar to Eq. (1). The tables and figures related to the adfreeze bond strength in the CSA guide are summaries

gathered from various experimental research papers and are available for specific soil types and pile materials. The SP 25.13330.2012 (2012)-based bearing capacity values are lower than those based on Weaver and Morgenstern (1981), which can be attributed to the more conservative frozen soil cohesion values suggested by the former. It is also of importance to mention that in North America, design factors of safety for geotechnical applications are higher than those in Russia (Streletskiy et al., 2012), which may justify the more conservative values assigned to the frozen soil cohesion in the Russian standards. For this study, the Russian procedure for estimating pile bearing capacity is chosen since the given tables for adfreeze bond values cover a wider range of ground temperatures and soil types.

Projected changes to the relevant climate variables are obtained by comparing the future 2021–2040 period with the current 1991–2010 period of the GEM4_CanESM2 simulation. Same approach is used to estimate future changes to pile bearing capacity and adfreeze contribution to pile bearing capacity based on GEM4_CanESM2 and offline CLASS simulations. For better estimation of bearing capacity for realistic pile scenarios such as those for bridges (in thick layer of sediments) used for river crossings, a site-level sensitivity analysis is performed for two locations; a northern and a southern location with bedrock at 41 m and 51 m depth, respectively, for 4 pile lengths (i.e., 5, 10, 15, and 20m piles). Following the conservative approach, the contribution of the pile tip as well as the friction within the active layer are neglected in the bearing capacity calculations in these sensitivity experiments. For consistency, the estimations are made for cement piles in these sensitivity experiments, even though CSA recommends steel piles for Northern Canadian regions. As discussed earlier, in the case of steel piles same equations are applicable, but with a reduction factor that yields adfreeze forces which are 30% smaller than that for cement piles.

3.3 Model Validation

Since the two important climate variables that influence permafrost are summer temperature and SWE, model ability in simulating these are presented first.

The spatial patterns of the mean summer 2m air temperatures simulated by GEM4_ERA5 are very similar to that of Daymet (Fig. 3.2a), with slight underestimations of up to 3°C.

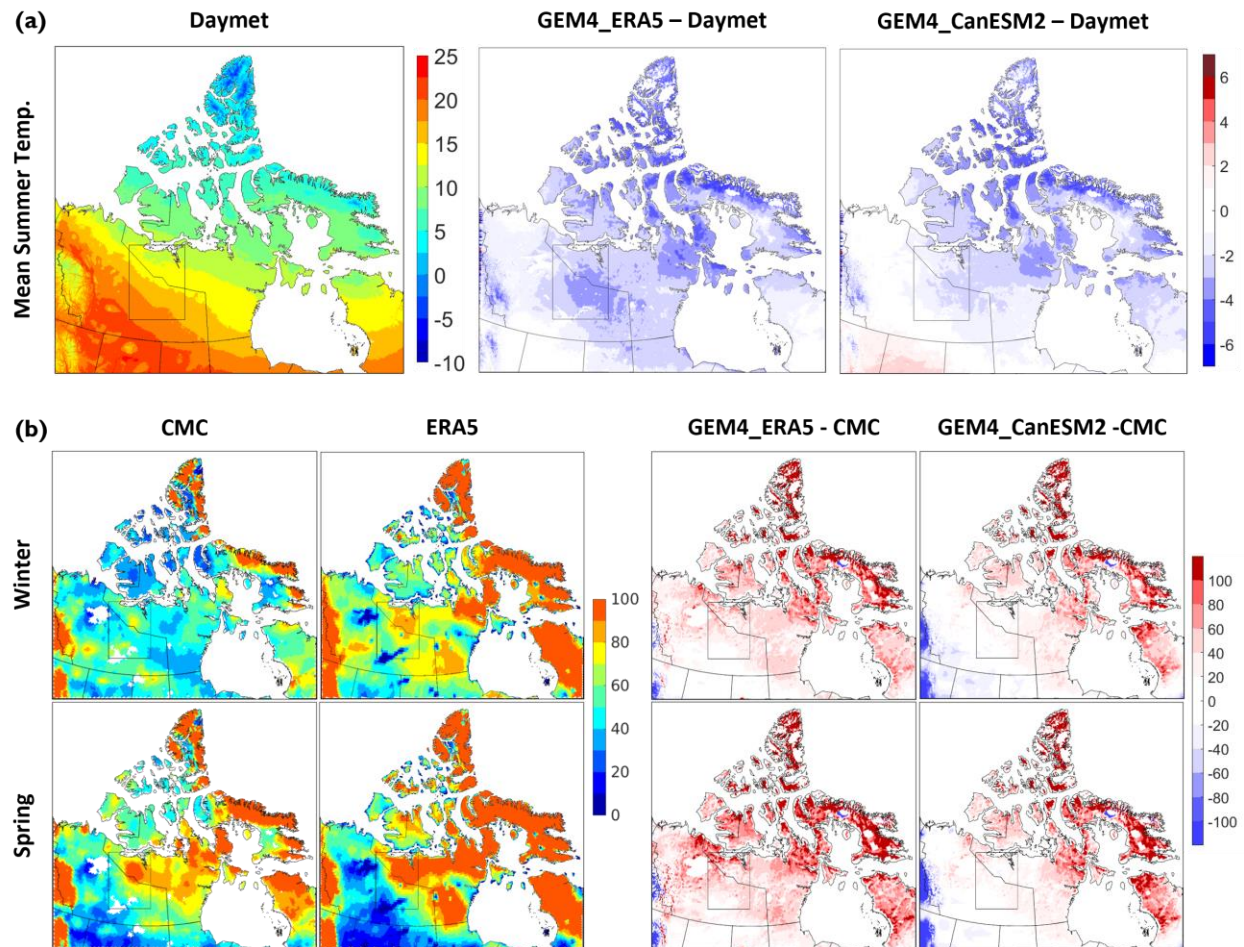


Figure 3.2 (a) Mean daily summer 2m air temperatures (in °C) for Daymet (left panel), and respective biases in GEM4_ERA5 (center panel), and GEM4_CanESM2 (right panel). (b) Mean winter (top row of panels) and spring (bottom row of panels) snow water equivalent (in mm) for CMC and ERA5 reanalysis, and biases in GEM4_ERA5, and GEM4_CanESM2 with respect to CMC.

GEM4_CanESM2 simulation results are also compared with Daymet and the differences reflect the combined performance and boundary forcing errors, the latter being due to errors in the

downscaled CanESM2 data. Results show similar patterns of temperature underestimations, compared to GEM4_ERA5, but with reduced magnitudes, which is due to the warm bias of CanESM2. GEM4_ERA5 simulated mean winter and spring snow water equivalent results are compared with those from ERA5 and CMC dataset, for the overlapping 2000-2010 period (Fig. 3.2b). It is important to note that there are significant differences between the two observation datasets, especially in the north-eastern regions, with ERA5 showing higher values. Compared to CMC, GEM4_ERA5 marginally overestimates SWE in the 20-60mm range, which when compared to ERA5 (figure not shown) is in the 20-80mm range for most regions within the domain. Given the large uncertainties in the observation datasets for the north-eastern regions, the overestimations noted in GEM4_ERA5 for these regions should be interpreted cautiously. It is also likely that GEM4_ERA5 captures SWE better due to the higher resolution compared to that of CMC. SWE in GEM4_CanESM2 has smaller values compared to GEM4_ERA5, and this is due to the warm bias in the driving CanESM2 data, as discussed earlier.

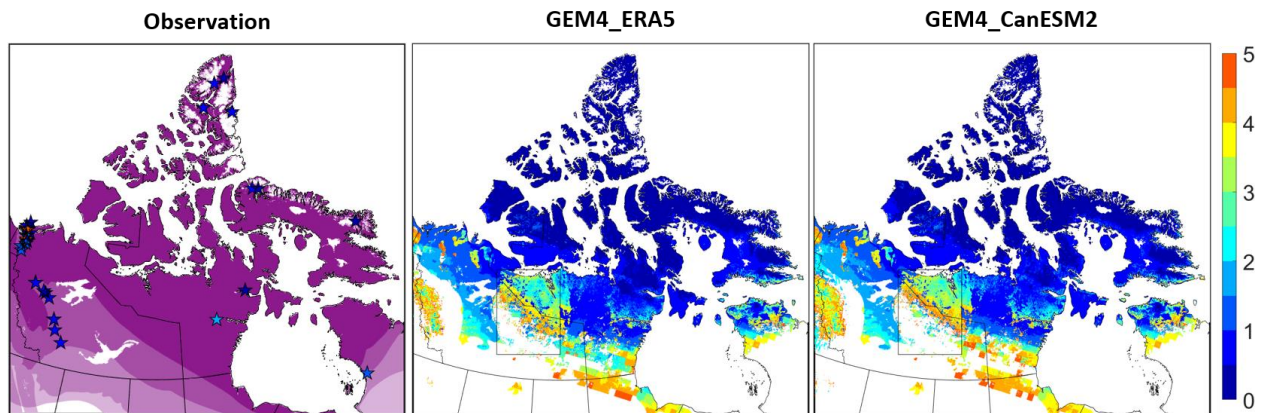


Figure 3.3 Observed mean ALT (m) for the 1991-2010 period (stars in the left panel). Also shown are the simulated ALT (for grid points with near-surface permafrost) from GEM4_ERA5 (center panel) and GEM4_CanESM2 (right panel) for the same period.

Comparison of the permafrost extent in Figure 3.3, shows that the model captures the continuous permafrost region relatively well, but fails to capture the near-surface permafrost, which is defined

in this study as permafrost in the top 5m, in the discontinuous zone, east of the Great Slave Lake and west of the Great Bear Lake. This is due to the lower values of depth to bedrock at the 4 km resolution of the model, that yields higher temperatures in the top 5 m of the soil, causing the permafrost table to be below 5 m. Taking that into consideration, the observed ALT values are compared with GEM4_ERA5 and GEM4_CanESM2 results in Fig 3.3, values are captured reasonably well by both simulations especially for the continuous permafrost region.

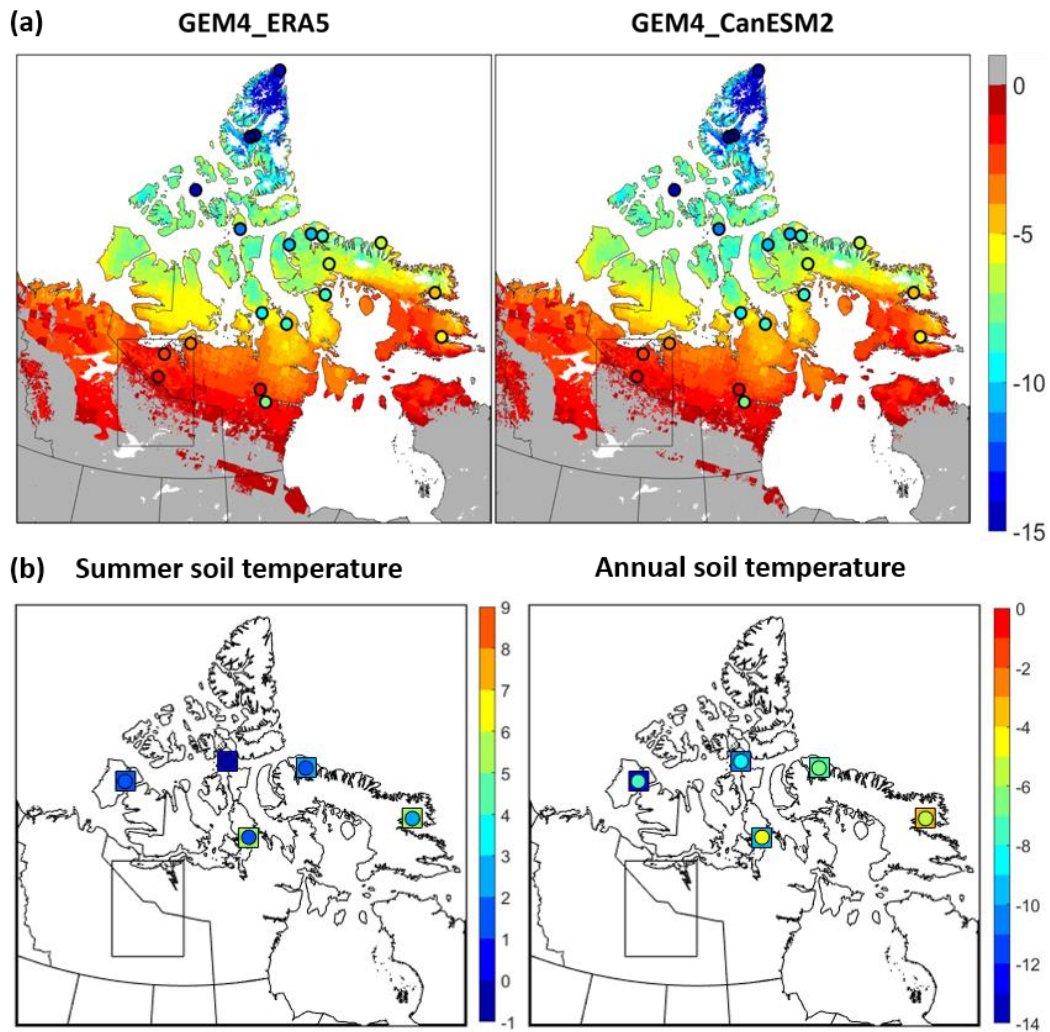


Figure 3.4 (a) soil temperature at 15-20m depth simulated by GEM4_ERA5 (left panel) and GEM4_CanESM2 (right panel); filled circles represent the observed soil temperature at the depth of zero annual amplitude. (b) Summer and annual soil temperatures at 0.5m depth (left and right panels, respectively); color filled circles indicate GEM4_ERA5 modeled soil temperatures and color filled squares represent the observed soil temperatures.

The observed soil temperatures at the depth of zero annual amplitude versus GEM4_ERA5 and GEM4_CanESM2 outputs are shown in Fig. 3.4a, MAGT values are captured reasonably well with biases less than 2°C for most points. Additionally, the annual and summer means of soil temperatures at 0.5-m depth at 5 locations from observation stations and GEM4_ERA5 outputs are compared in Fig. 3.4b, annual and summer means are captured very well by GEM4_ERA5, with noticeable underestimations (3-4°C) at two sites only. Biases in soil temperature can be attributed to the land geomorphology where different surface vegetations and manmade landscapes cannot be accurately represented in a 4-km grid cell, especially when the observation stations are mostly located in airports (Boreholes 281, and 1148).

The study of bearing capacity in permafrost regions necessitates the understanding of several contributing factors (i.e., the depth to bedrock, soil composition, frozen moisture content, and thermal regime). Although the bedrock for the studied region can locally be as deep as 50 m, according to ORNL DAAC database (Pelletier et al., 2016), the average depth to bedrock at 4km resolution varies between 0 and 5 m (Fig. 3.1c). A 5 m pile is therefore selected for the analysis. In terms of the land model configuration in GEM, the top 5 m is divided into 12 layers as mentioned in section 3.2.1.

For the current 1991-2010 period, the estimated ALT for regions with simulated near-surface permafrost ranges between 0-5m (Fig. 3.5), with the highest values occurring at the southernmost regions of the continuous permafrost, while the ALT in northern regions is mostly less than 1m. For the adfreeze force, results show that values can be as high as 2000 kN, accounting for more than 70% of the total bearing capacity, in regions with cooler soils and deeper bedrock; This is due to the larger values suggested for R_{af} (see Eq. (1)) for colder permafrost, and the larger area of contact (A_{af}) between the pile and permafrost. Less than 250kN adfreeze force is obtained for the

Slave Geological-Grays Bay Corridor based on data at 4 Km resolution, which uses shallow depth to bedrock and has higher soil temperatures especially in the southern half of the corridor. Detailed ground modelling, driven by the 4 km simulation outputs, can be useful in capturing the ground thermal and moisture regimes realistically, as discussed in Section 3.5. Results obtained from GEM4_ERA5 and GEM4_CanESM2 simulations are very similar for ALT, adfreeze force, and the total bearing capacity. Although the adfreeze force seems to be low across the corridor, the total bearing capacity shows very high values coming from the bedrock bearing. The estimated total bearing capacity values, range from less than 500 kN, in regions with deep bedrock and warm soils, to 8000-10000 kN in colder grounds with shallower bedrock.

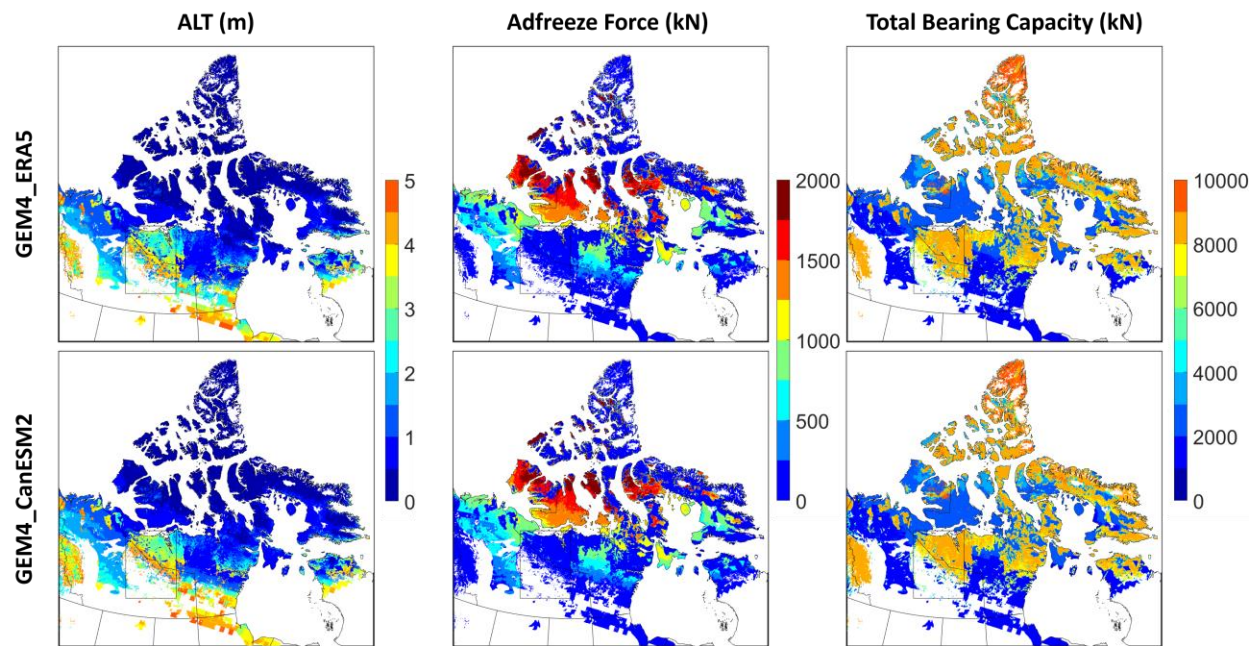


Figure 3.5 The active layer thickness (ALT, in m; left panels), adfreeze force (in kN; center panels), and total bearing capacity (in kN; right panels) estimated using GEM4_ERA4 (top panels) and GEM4_CanESM2 (bottom panels).

3.4 Projected changes to pile bearing capacity and related climate variables

Before presenting projected changes to pile bearing capacity, projected changes to relevant climate variables are presented. The projected changes to summer mean temperatures shown in Fig. 3.6a,

suggest increases of up to 3°C, with some regions showing 4°C increase, for the 2021-2040 period compared to the 1991-2010 period. This increase in summer temperature can increase ALT.

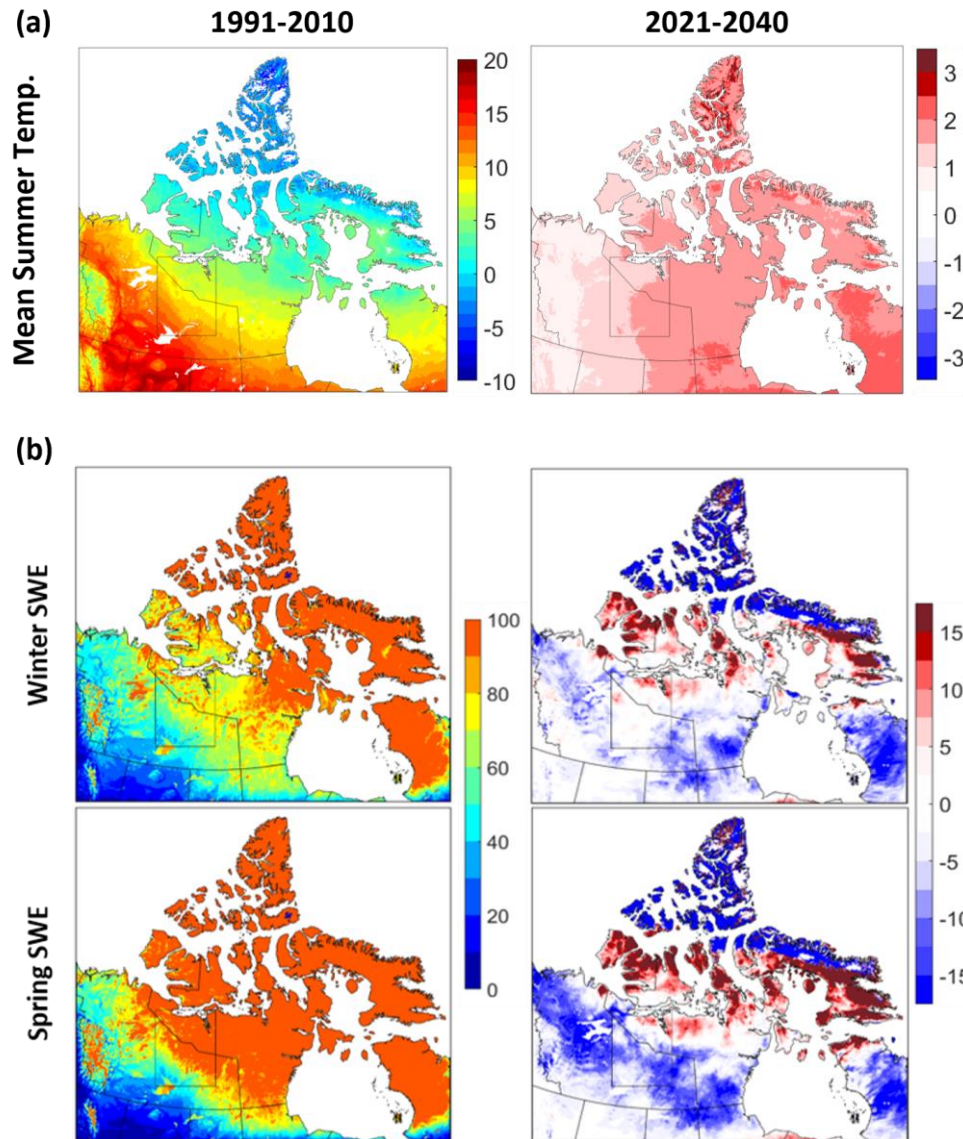


Figure 3.6 (a) Mean daily summer 2m air temperature (in °C) for the current 1991-2010 period (left panel) and projected changes for the future 2021-2040 period (right panel). (b) Mean winter snow water equivalent, in mm, (top panels) and mean spring snow water equivalent (bottom panels) for the current period (left panels) and respective projected changes for the future period (right panels).

The projected changes to SWE shown in Fig. 3.6b, suggest increases in winter SWE with values up to 20mm for the region enclosed between 65° N and 73° N latitudes and decreases with similar values are noted for regions north and south of this latitudinal band. Spring SWE is projected to

follow the same pattern and values, with changes covering larger areas in the domain. Even though decreases in SWE noted outside of the 65°N-73°N latitudinal band can contribute to decreasing ALT, inspection of the projected changes to ALT (Fig. 3.7) indicates that the increase in summer temperature is dominant, leading to an overall increase in ALT.

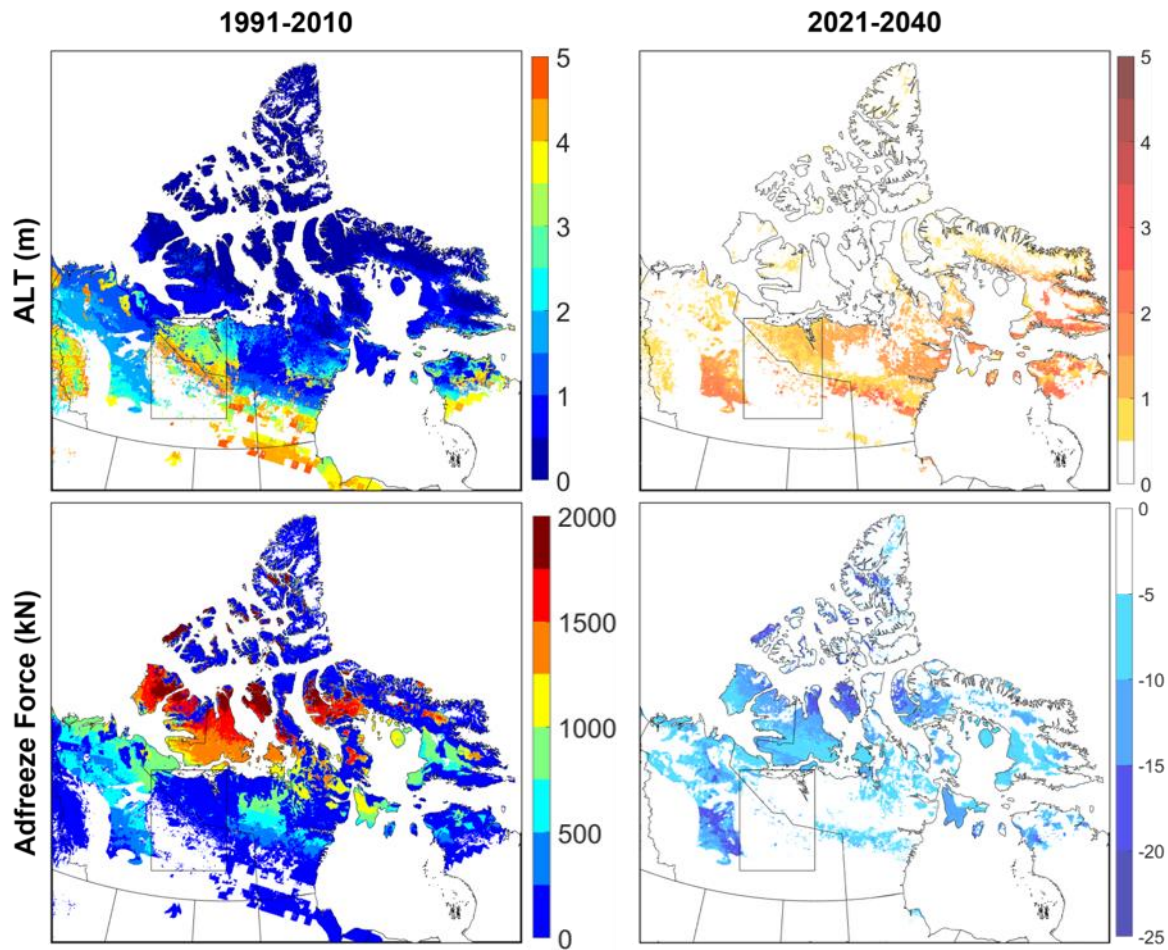


Figure 3.7 The estimated ALT (top row) and adfreeze force (bottom row) from GEM4_CanESM2 for the 1991-2010 period (left column) and the respective projected changes for the 2021-2040 period (right column).

Comparing the results for the studied periods, modest changes can be noticed in terms of the total bearing capacity and that is due to the significant bearing of the bedrock where present. The projected changes to the ALT show an increase in the order of 1-3m for the southern part of the continuous permafrost region for the 2021-2040 period, resulting in the complete disappearance

of permafrost in the top 5 m of the ground for the southmost regions of the continuous permafrost and transitional zones, while the northernmost regions are estimated to experience less than 0.5m increase in the ALT. This increase in ALT results in reduced A_{af} , leading to decreases in the adfreeze force. The projected changes to the adfreeze force (%) suggest, as expected, that regions with deeper bedrock are projected to be the most affected. The analysis for 2021-2040 period suggests a 10-20% decrease for regions with shallower bedrock and regions in the middle of the continuous permafrost, and up to 30% for regions with deeper bedrock and closer to the southern edge of the continuous permafrost (along the Mackenzie River valley).

For the southern regions, results suggest decreases of up to 30% in the summer ground frozen moisture content by 2040, which can lead to reduced ground stability in the form of thaw settlements, while the projected decreases are less than 15% for northern permafrost regions (figure not shown). The translation from ice rich to ice poor state could indicate an improvement in the adfreeze bond. However, results show that this translation is accompanied with increases in the soil temperatures and ALT that will lead to reductions in the adfreeze bond strength, especially with the conservative approach followed where the potential frictional strength within the active layer is neglected.

3.5 Slave Geological-Gray's Bay Corridor

As discussed in section 3.2.1, new future developments including an all-season road planned for this corridor warrants detailed analysis. Super resolution (250 m) offline simulations are therefore performed with the land model of GEM, i.e., CLASS, to better capture the ground heterogeneity and thus thermal and moisture regimes. These simulations are driven by GEM4_CanESM2 outputs. The surface heterogeneity, including the depth to bedrock, especially around water bodies is more realistically represented at 250m resolution as shown in figure 8a. The added value of the

super-resolution simulation is particularly reflected in its ability to capture the near-surface permafrost for the southern region of the corridor, i.e., the east of the Great Slave Lake, which was not captured in the GEM simulation (Fig. 3.8b).

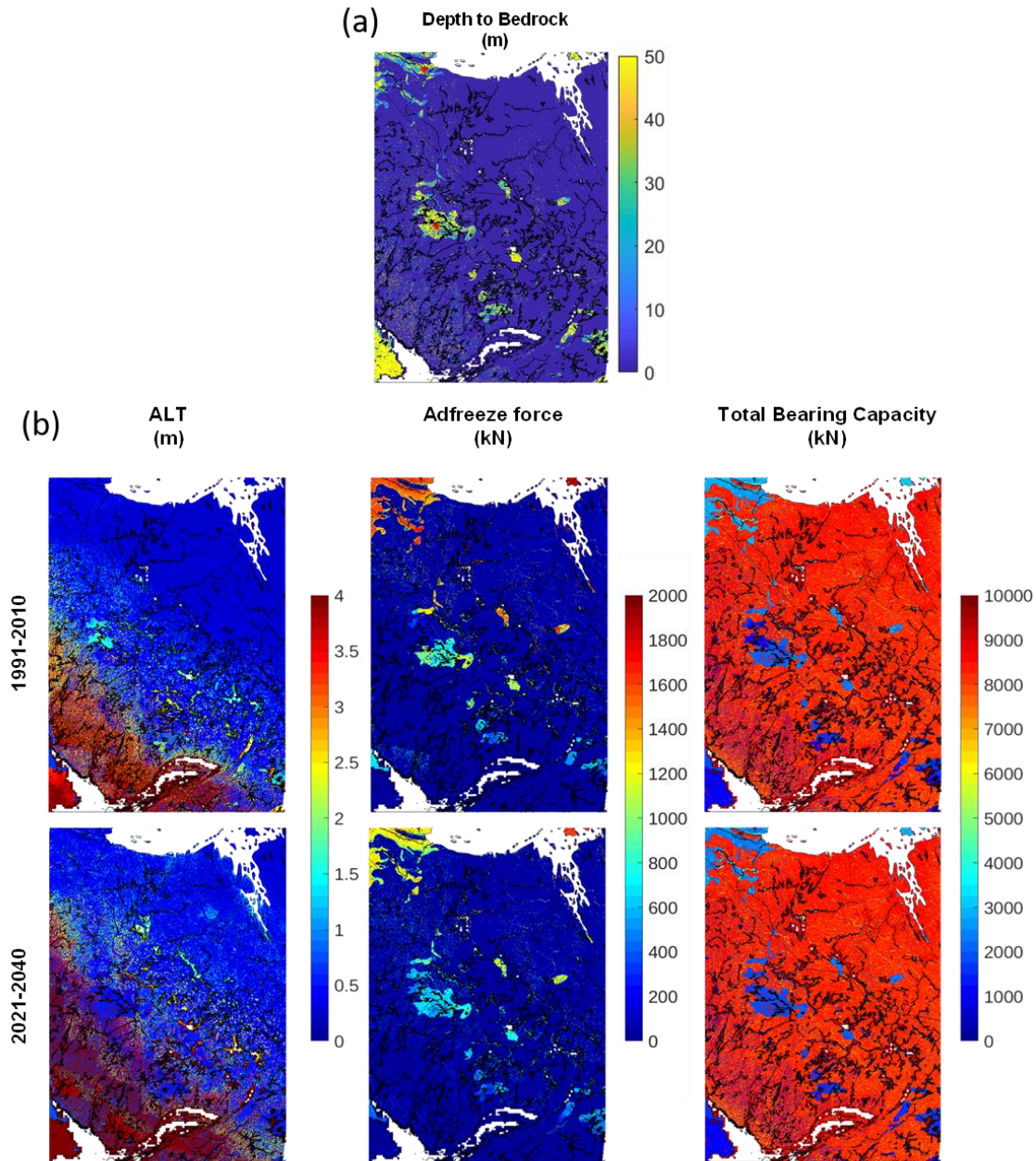


Figure 3.8 (a) Depth to bedrock (m) at 250 m resolution; red asterisks show the location of the points used for the sensitivity analysis presented in Fig. 10 and 11. (b) ALT (m), Adfreeze force (kN), and total bearing capacity (kN) at 250-m resolution, over the Slave Geological-Grays Bay Corridor, for the 1991-2010 (top figures) and 2021-2040 (bottom figures) periods.

Furthermore, the illustrated pattern defines the boundary between the continuous and discontinuous permafrost realistically, which suggests great improvements to ground thermal modelling. For the current period (1991-2010), the ALT around the Great Slave Lake ranges from less than 0.5m to 4m, which agrees particularly with observations of lowlands permafrost in the Great Slave region (Paul et al., 2020). As can be seen in Fig. 8b, the adfreeze force reaches values as high as 1800 kN in regions with deep bedrock in the northern parts of the domain, while the values in the discontinuous permafrost regions are less than 1000 kN. The total bearing capacity estimated for the 5m cement pile show little changes. For the future period (2021-2040), projected changes to the ALT, shown in Fig. 3.9, suggest increases to be as high as 4 meters around the Great Slave Lake and regions in the discontinuous permafrost, while Northern regions in the continuous permafrost are estimated to have less than 1-m increase in the ALT.

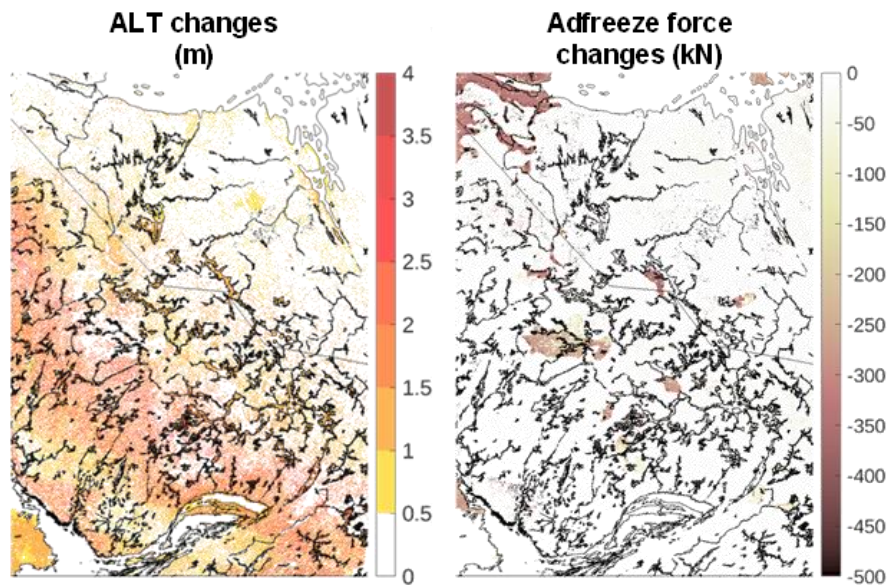


Figure 3.9 Projected changes to the ALT (m), and adfreeze force (kN) for the Slave Geological-Grays Bay Corridor for the 2021-2040 period respective to 1991-2010 period at 250 m resolution.

In terms of the adfreeze force, results for 2021-2040 period suggests decreases up to 300-kN for regions with shallower bedrock and regions in the continuous permafrost, and up to 600-kN for regions with deeper bedrock and closer to the southern edge of the continuous permafrost.

To reflect realistic possible scenarios, such as in the case of bridges across rivers, with possibly thick sediment deposits and therefore deeper bedrocks, other pile configurations are considered for a northern and a southern point (locations are marked in Fig 3.8a).

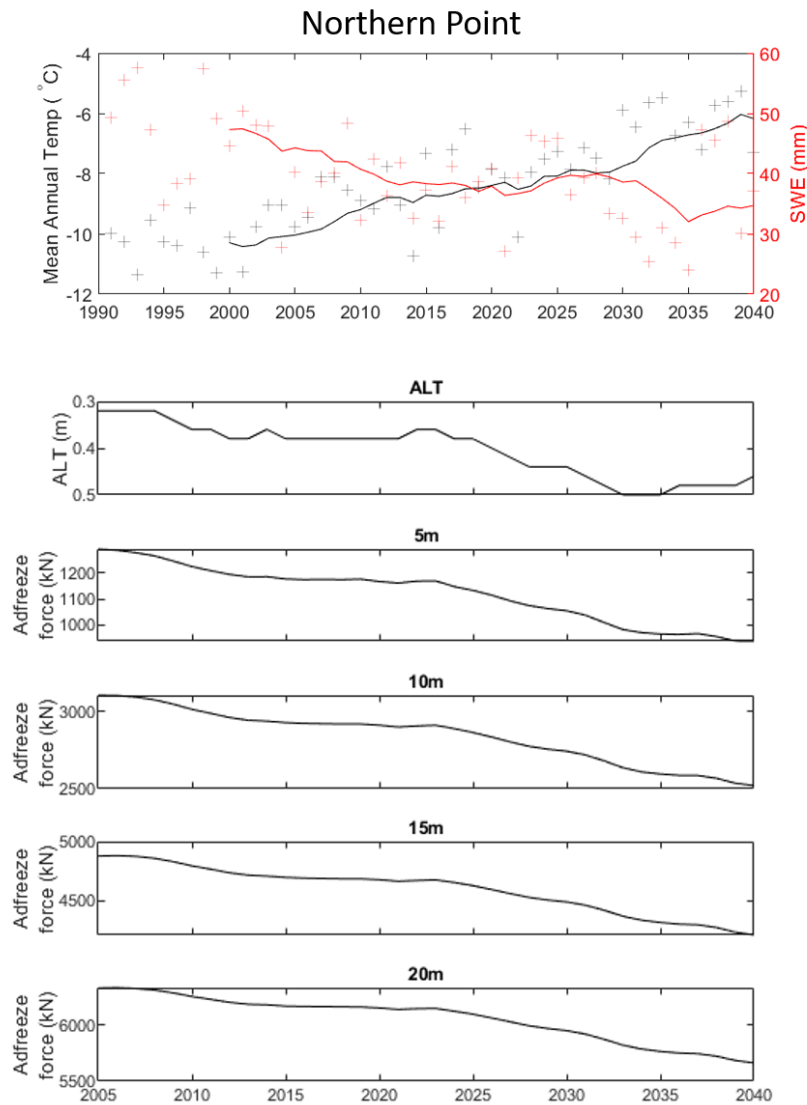


Figure 3.10 The 10-year running average of the mean annual temperature (in black) and SWE (in red) obtained from GEM4_CanESM2 with the yearly values shown by a '+' sign. The ALT (m) and adfreeze force (in kN for four different pile scenarios; 5, 10, 15, and 20-m) timeseries for the Northern point.

Figure 3.10 shows a 10-year running average of the ALT and adfreeze force for four pile scenarios, i.e., for pile lengths of 5m, 10m, 15m, and 20m, for the northern point. The ALT increase from 0.3 to 0.5 meters with the steepest decrease occurring after 2025 for this location. In terms of the adfreeze force, results indicate decreases between 20-25% for shorter piles (5, and 10m), and 8-12% for longer piles, since deeper permafrost temperatures are more stable.

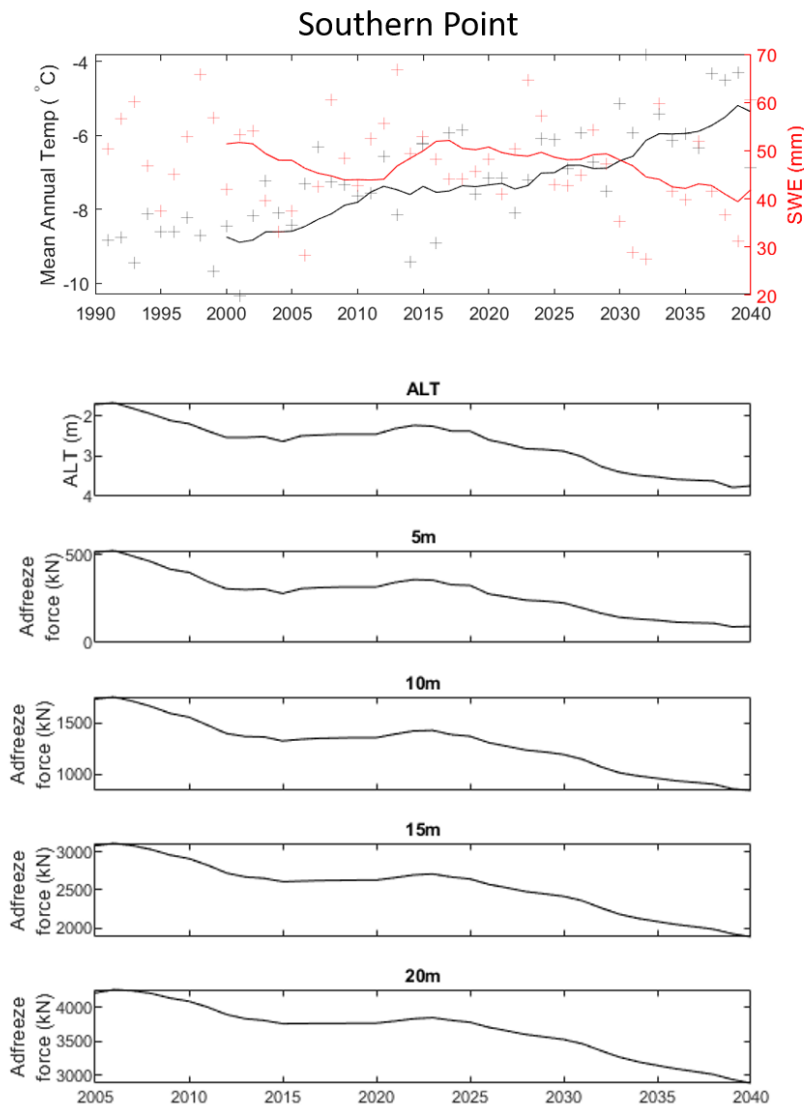


Figure 3.11 The 10-year running average of the mean annual temperature (in black) and SWE (in red) obtained from the GEM4_CanESM2 with the yearly values shown by a '+' sign. The ALT (m) and adfreeze force (in kN for four different pile scenarios; 5, 10, 15, and 20-m) timeseries for the Southern point.

For the southern point in the discontinuous permafrost region (Fig. 3.11), larger changes than for the northern point are expected. The ALT increase from 1.8 to 3.9 meters with a steep decreasing trend post 2025. Results indicate more abrupt decreases in the adfreeze force, compared to the northern point, in the 28-35% range for longer piles (15, and 20m), the 10m pile is estimated to lose about 45% of its adfreeze force, while the 5-meter pile will lose over 85% capacity by the end of the studied period.

3.6 Summary and conclusions

The potential climate warming consequences on pile bearing capacity, for the eastern Canadian Arctic are evaluated for the future 2021-2040 period, relative to 1991-2010 period, using a 4km high-resolution climate simulation corresponding to RCP8.5 scenario, over the region for the very first time. Comparison of summer air temperature, snow water equivalent, soil temperature, and active layer thickness, which influence pile bearing capacity, from the ERA5-driven GEM simulation with available observation datasets confirms the ability of the model in simulating climate characteristics. Slightly higher values of summer temperatures and lower values of SWE are seen in the CanESM2-driven GEM simulation for current climate, which is associated with the warm-bias in the driving CanESM2 data.

Results for the future 2021-2040 period suggest increases to summer temperatures in the 1-3°C range for the entire domain, while SWE is projected to increase for the latitudinal band enclosed by 65°N and 73°N, ranging between 5-20mm, and decrease everywhere else with similar range. The combined effect is reflected in ALT increases in the 1-3m range which will lead to an active layer thickness of up to 5 meters around the continuous-to-discontinuous permafrost transitional zone. For the cement pile of 5m length considered, on a regional scale, mean decreases in the adfreeze force are found to be in the 5-30% range.

Additional super-resolution (250 m) offline simulation with the land model in GEM, provide detailed information for the Slave Geological-Grays Bay Corridor, which manages to capture near-surface permafrost regions that were missed in the GEM simulation at 4 km. ALT ranged from 0-4m within the corridor and is projected to increase with values reaching 4 m in the discontinuous permafrost region, while the adfreeze force for the corridor, which shows values around 250-kN at 4 km resolution, is estimated to be as high as 1800 kN and is estimated to have reductions in the 300-600 kN range. Furthermore, site-level sensitivity experiments performed for the two locations for different pile lengths shed important insights: larger decreases in the adfreeze force for piles in regions with deeper bedrock and warmer permafrost, with up to 45% reduction for longer piles and 85% reduction for shorter piles by the end of 2040. Streletskiy et al. (2012) and Shiklomanov et al. (2017) in their study focused over Russian permafrost regions also reported important decreases in bearing capacity in the southmost regions of the continuous permafrost with similar range of projected decreases. The super-resolution simulation outputs are shown to add a significant value to the analysis in the form of thorough surficial details that recognize rivers, small lakes, and deep sediment layers around them, in addition to a more realistic ALT and soil temperature estimations due to the finer layering of the soil column. The regional-scale analysis and results presented here for the first time can inform future developments as well as existing infrastructure.

Due to the high computational cost involved in undertaking the high-resolution GEM simulations, the study was able to consider only one emission scenario and one driving GCM. To better quantify the uncertainties in climate projections, a multi-model ensemble at 4 km resolution, or at the very least an ensemble driven by different members of a GCM such as CanESM2 is needed. In addition, future studies are contingent on the chosen emission scenario. Therefore, additional studies on the

bearing capacity and permafrost thermal state using climate simulations for different emission scenarios should be undertaken.

Moreover, the simulations considered in this study assume free drainage at the bottom of the soil column, this might not be realistic everywhere, and experiments with reduced drainage can be useful for better understanding. Furthermore, abundant ground ice is not integrated in the land model of GEM which leads to underestimations of the soil frozen moisture content over some regions as discussed in Teufel and Sushama (2019). Also, the validation of the performed simulations is limited by the lack of observed data, especially soil temperatures and ALT, in Canada's North, and therefore more efforts will be required to address this issue. Nonetheless, the convection permitting climate simulations undertaken here are important for engineering planning, management, and operations, and will provide the basis for future studies.

CHAPTER 4 - CONCLUSIONS AND RECOMMENDATIONS

4.1 Conclusions

This thesis presents the projected changes to the bearing capacity of pile foundations in a warmer climate across the eastern Arctic region of Canada, more specifically over Nunavut and the NWT. Increases in soil temperatures lead to increases in the active layer thickness which in turn can result in catastrophic consequences on the stability of infrastructure supported on permafrost. Different experiments are performed over the region to better understand the evolution of the bearing capacity of piles of different lengths, which are based on the soil temperatures obtained from the very first convection-permitting GEM simulation over the region, at 4-km resolution, for the current 1991-2010 and future 2021-2040 periods for RCP8.5 emission scenario and an offline land only simulation performed over the Slave Geological-Grays Bay Corridor, at 250-m horizontal resolution. Validation of GEM simulated permafrost-related variables confirms the ability of the model in simulating most of the variables very well with limited biases noted over some locations. This gives confidence in applying the model to assess the changes to the bearing capacity of pile foundations in future climate.

The findings of this research suggest increases to summer temperatures in the 2-3°C range over the study region for the 2021-2040 period, while winter and spring snow water equivalent are projected to increase by 15mm for the regions enclosed between 65° N and 73° N latitudes and decreases with similar values are noted for regions north and south of this latitudinal band. With a note that the model captures the entire extent of the continuous permafrost and transitional zones to the discontinuous extent, subsequent analysis indicates large increases to the active layer thickness (1-3 m) for many regions of the study domain. Increases in ALT and permafrost temperature result in reductions to the adfreeze force that are as high as 30% for the southern

regions with warmer permafrost and relatively deep bedrock. Changes to regions underlain by deep bedrock are the most critical from structural stability point of view as the adfreeze force contribution to the total bearing capacity can be up to 70% in such regions.

The super-resolution offline simulation (250 m) demonstrates significant added value to the study as it captures changes to the ground thermal regime in regions in the discontinuous permafrost that were missed by the 4-km GEM simulations, brought by the better representation of surface heterogeneity. Spatially, the analysis results agree with the findings of the 4-km experiment in the continuous permafrost region, while the discontinuous permafrost region is expected to witness larger decrease in terms of the active layer thickness (up to 4m).

The sensitivity analysis over two selected points provides the opportunity to consider different lengths of piles (i.e., 5, 10, 15, and 20-m) embedded in regions with very deep bedrock, as in the case of piles (in thick sediments) used for supporting bridges used for river crossings. Results for the adfreeze force indicate reductions in the 8-25% range for piles for a northern more stable permafrost region, with shorter piles showing the most critical reductions, as expected, while the piles located in the warmer southern region in the discontinuous permafrost are estimated to lose 28-85% of their capacity by the end of 2040.

This study is the first contribution to the investigation of pile bearing capacity evolution through ultra-high-resolution climate modelling for the eastern Canadian permafrost region.

4.2 Limitations and future research

The main limitations of this study that can be addressed in future work are discussed here.

The GEM transient climate change simulations were only performed until 2040 due to high computational costs. To better quantify uncertainties in future projections, multi-model ensembles or at the very least an ensemble of simulations driven by different members of a GCM are required.

Furthermore, other emission scenarios should be considered in future studies. Additionally, since GEM simulations at 4 km horizontal resolution are expensive to run, experiments using the land model in GEM can be used to advance ground-related outputs. However, it is essential to couple the land model with reliable high-resolution geophysical fields to better simulate changes to permafrost.

Model improvements in regions with ice-rich soils are required. O'Neil et al. (2019) generated a new ground ice map for Canada using a paleogeographic modelling approach, and more efforts are needed to incorporate such information into GEM simulations. Also, the simulations used for this study assume free drainage at the bottom of the soil column which might not be realistic everywhere within the domain. Experiments with reduced drainage can be valuable in understanding the impact of bottom drainage on changes to permafrost modeling. Furthermore, the lack of observed data in Canada's Arctic hinders the validation of the model simulated ground fields, and future efforts to develop dense monitoring are recommended

It must be noted that the findings reported in this study serve as a general indicator to the expected impacts of climate warming on pile bearing capacity on a regional scale and can not be directly applied to a particular site due to the wide variation of pile materials, lengths, installation methods, and on-site soil properties. However, the framework developed in this study, when coupled with site-specific geophysical parametrizations, can be substantially informative for many engineering applications and valuable for adaptation related decision-making.

REFERENCES

- Andersland, O. and Ladanyi, B., 1994. *An Introduction to Frozen Ground Engineering*. New York: Chapman and Hall, pp.77-78.
- Andersland, O. B., and Ladanyi, B. (2003). *Frozen ground engineering*. John Wiley and Sons.
- Armstrong, E., Hopcroft, P. O., and Valdes, P. J. (2019). Reassessing the value of regional climate modeling using paleoclimate simulations. *Geophysical Research Letters*, 46(21), 12464-12475.
- Bélair, S., Mailhot, J., Girard, C., and Vaillancourt, P. (2005). Boundary layer and shallow cumulus clouds in a medium-range forecast of a large-scale weather system. *Monthly weather review*, 133(7), 1938-1960.
- Benoit, R., Côté, J., and Mailhot, J. (1989). Inclusion of a TKE boundary layer parameterization in the Canadian regional finite-element model. *Monthly weather review*, 117(8), 1726-1750.
- Brooks, H., Doré, G., and Locat, A. (2021). Soil Bridging Effects within Permafrost-Supported Embankment Infrastructure. *Journal of Cold Regions Engineering*, 35(1), 04020027.
- Brown, J., Hinkel, K. M., and Nelson, F. E. (2000). The circumpolar active layer monitoring (CALM) program: research designs and initial results. *Polar geography*, 24(3), 166-258.
- Brown, R. (1964). Guide for Design and Construction of Pile Foundations in Permafrost. *Nrc Div Bldg Res Tech Transl/Can/*.
- Brown, R., and Brasnett, B. (2010). Updated annually. *Canadian Meteorological Centre (CMC) daily snow depth analysis data*. Boulder, Colorado USA: NASA DAAC at the National Snow and Ice Data Center.
- Cheng, G., Zhang, J., Sheng, Y., and Chen, J. (2004). Principle of thermal insulation for permafrost protection. *Cold Regions Science and Technology*, 40(1-2), 71-79.
- Clarke, E. S. (Ed.). (2007, September). *Permafrost Foundation: State of the Practice*. American Society of Civil Engineers.
- Côté, J., Gravel, S., Méthot, A., Patoine, A., Roch, M., and Staniforth, A. (1998). The operational CMC-MRB global environmental multiscale (GEM) model. Part I: Design considerations and formulation. *Monthly weather review*, 126(6), 1373-1395.
- Couture, R., Robinson, S. D., and Burgess, M. (2000). *Climate change, permafrost degradation, and infrastructure adaptation: preliminary results from a pilot community case study in the Mackenzie valley*. Geological Survey of Canada Ottawa, ON.
- CRORY, F. E. 1963. Pile foundations in permafrost. *Proceedings, 1st International Conference on Permafrost*, Lafayette, pp. 467-476.

CSA. Canadian Standards Association, 2019, Technical Guide: Infrastructure in permafrost: A guideline for climate change adaptation: Canadian Standards Association Group, CSA PLUS 4011:19, 91 p.

Darrow, M. M. (2011). Thermal modeling of roadway embankments over permafrost. *Cold Regions Science and Technology*, 65(3), 474-487.

Delage, Y. (1997). Parameterising sub-grid scale vertical transport in atmospheric models under statically stable conditions. *Boundary-Layer Meteorology*, 82(1), 23-48.

Dennison, P. P. (2017). *Understanding and Developing Estimates Based on Practical Foundation Methods for Alaska's Discontinuous Permafrost Region*.

Diaconescu, E. P., Laprise, R., and Sushama, L. (2007). The impact of lateral boundary data errors on the simulated climate of a nested regional climate model. *Climate dynamics*, 28(4), 333-350.

Diro, G. T., and Sushama, L. (2019). Simulating Canadian Arctic climate at convection-permitting resolution. *Atmosphere*, 10(8), 430.

Dukhan, T., and Sushama, L. (2021). Understanding and modelling future wind-driven rain loads on building envelopes for Canada. *Building and Environment*, 196, 107800.

Esch, D. C. (2004). Thermal analysis, construction, and monitoring methods for frozen ground. American Society of Civil Engineers.

Farouki, O., 1992. European foundation designs for seasonally frozen ground. Monograph 92-1. U.S. Army Corps of Engineers, Cold Regions Res. and Engineering Lab., Hanover, N.H.

Fernandez Santoyo, S., Tom Jr, J. G., and Baser, T. Impact of Subsurface Warming on the Capacity of Helical Piles Installed in Permafrost Layers. In IFCEE 2021 (pp. 239-248).

Gao, Q., Wen, Z., Ming, F., Liu, J., Zhang, M., and Wei, Y. (2019). Applicability evaluation of cast-in-place bored pile in permafrost regions based on a temperature-tracking concrete hydration model. *Applied Thermal Engineering*, 149, 484-491.

Giorgi, F. (2019). Thirty years of regional climate modeling: where are we and where are we going next?. *Journal of Geophysical Research: Atmospheres*, 124(11), 5696-5723.

Goering, D. J. (1998, June). Experimental investigation of air convection embankments for permafrost-resistant roadway design. In Proceedings of 7th International Conference on Permafrost (Vol. 326). Yellowknife, Canada, Nordicana, Quebec.

Goosse, H., Kay, J. E., Armour, K. C., Bodas-Salcedo, A., Chepfer, H., Docquier, D., Jonko, A., Kushner, P. J., Lecomte, O., and Massonnet, F. (2018). Quantifying climate feedbacks in polar regions. *Nature communications*, 9(1), 1-13.

GTN-P (2015): Global Terrestrial Network for Permafrost metadata for permafrost boreholes (TSP) and active layer monitoring (CALM) sites. PANGAEA,

<https://doi.org/10.1594/PANGAEA.842821>, Supplement to: Biskaborn, Boris K; Lanckman, Jean-Pierre; Lantuit, Hugues; Elger, Kirsten; Streletskiy, Dmitry A; Cable, William L; Romanovsky, Vladimir E (2015): The new database of the Global Terrestrial Network for Permafrost (GTN-P). *Earth System Science Data*, 7(2), 245-259, <https://doi.org/10.5194/essd-7-245-2015>

Harries, C. (2018). Review of Current Practice of Building Foundations in the Canadian North. Cold Climate HVAC Conference,

Hersbach, H., Bell, B., Berrisford, P., Hirahara, S., Horányi, A., Muñoz-Sabater, J., Nicolas, J., Peubey, C., Radu, R., and Schepers, D. (2020). The ERA5 global reanalysis. *Quarterly Journal of the Royal Meteorological Society*, 146(730), 1999-2049.

Hoeve, T. E., and Trimble, J. R. (2018). Rationalizing the design of adfreeze piles with limit states design. *GeoEdmonton 2018*.

Holubec, I. (2008). *Flat loop thermosyphon foundations in warm permafrost*. Government of the Northwest Territories Asset Management Division of Public Works and Services and the Climate Change Vulnerability Assessment of the Canadian Council of Professional Engineers.

Huang, J., McCartney, J. S., Perko, H., Johnson, D., Zheng, C., and Yang, Q. (2019). A novel energy pile: The thermo-syphon helical pile. *Applied Thermal Engineering*, 159, 113882.

IPCC (2019). Climate Change and Land: an IPCC special report on climate change, desertification, land degradation, sustainable land management, food security, and greenhouse gas fluxes in terrestrial ecosystems [P.R. Shukla, J. Skea, E. Calvo Buendia, V. Masson-Delmotte, H.-O. Pörtner, D. C. Roberts, P. Zhai, R. Slade, S. Connors, R. van Diemen, M. Ferrat, E. Haughey, S. Luz, S. Neogi, M. Pathak, J. Petzold, J. Portugal Pereira, P. Vyas, E. Huntley, K. Kissick, M. Belkacemi, J. Malley, (eds.)]. In press.

IPCC (2021). Climate Change 2021: The Physical Science Basis. Contribution of Working Group I to the Sixth Assessment Report of the Intergovernmental Panel on Climate Change [Masson-Delmotte, V., P. Zhai, A. Pirani, S.L. Connors, C. Péan, S. Berger, N. Caud, Y. Chen, L. Goldfarb, M.I. Gomis, M. Huang, K. Leitzell, E. Lonnoy, J.B.R. Matthews, T.K. Maycock, T. Waterfield, O. Yelekçi, R. Yu, and B. Zhou (eds.)]. Cambridge University Press. In Press.

Jeong, D. I., and Sushama, L. (2019). Projected changes to mean and extreme surface wind speeds for North America based on regional climate model simulations. *Atmosphere*, 10(9), 497.

Johnston, G. H. (1963). Pile construction in Permafrost. *Nrc Div Bldg Res Tech Papers/Can/*.

Johnston, G. H. (1981). *Permafrost: engineering design and construction*. Toronto, NewYork: Wiley.

Kain, J. S., and Fritsch, J. M. (1990). A one-dimensional entraining/detraining plume model and its application in convective parameterization. *Journal of Atmospheric Sciences*, 47(23), 2784-2802.

Korhonen, C. J., and Brook, J. W. (1996). Freezing temperature protection admixture for portland cement concrete.

Li, G., Yu, Q., Ma, W., Chen, Z., Mu, Y., Guo, L., and Wang, F. (2016). Freeze–thaw properties and long-term thermal stability of the unprotected tower foundation soils in permafrost regions along the Qinghai–Tibet Power Transmission Line. *Cold Regions Science and Technology*, 121, 258-274.

Li, J., and Barker, H. (2005). A radiation algorithm with correlated-k distribution. Part I: Local thermal equilibrium. *Journal of the atmospheric sciences*, 62(2), 286-309.

Li, N., and Xu, B. (2008). A new type of pile used in frozen soil foundation. *Cold Regions Science and Technology*, 53(3), 355-368.

Liu, Z.-Y., Cui, F.-Q., Chen, J.-B., Jin, L., Wang, W., and Zhang, W. (2020). Study on the permafrost heat transfer mechanism and reasonable interval of separate embankment for the Qinghai-Tibet expressway. *Cold Regions Science and Technology*, 170, 102952.

Martynov, A., Sushama, L., and Laprise, R. (2010). Simulation of temperate freezing lakes by one-dimensional lake models: performance assessment for interactive coupling with regional climate models.

Miller, D. and Johnson, L., (2000). Pile Settlement in Saline Permafrost - A Case History. PERMAFROST - CANADA Proceedings of the Fifth Canadian Permafrost Conference. pp.371-378.

Mironov, D., Golosov, S., Heise, E., Kourzeneva, E., Ritter, B., Sceider, N., and Terzhevik, A. (2005). Flake-a lake model for environmental applications. Proc. of the 9th Workshop on Physical Processes in Natural Waters,

National Research Council Canada. Division of Building Research, Porkhaev, G. V., Vialov, S. S., and Nauchno-issledovatel'skii institut osnovanii i podzemnykh sooruzhenii (Akademiia stroitel'stva i arkhitektury SSSR). (1976). *Handbook for the design of bases and foundations of buildings and other structures on permafrost*. Canada Institute for Scientific and Technical Information.

National Research Council of Canada (NRCC). (1976). Handbook for the design of bases and foundations of buildings and other structures on permafrost. NRC TT-1865, Ottawa, Ont., 141 p.

Nelson, F. E., Anisimov, O. A., and Shiklomanov, N. I. (2001). Subsidence risk from thawing permafrost. *Nature*, 410(6831), 889-890.

Nikiforova, N. S., and Konnov, A. V. (2021, June). Influence of permafrost degradation on piles bearing capacity. In *Journal of Physics: Conference Series* (Vol. 1928, No. 1, p. 012046). IOP Publishing.

Oh, S. G., and Sushama, L. (2020). Short-duration precipitation extremes over Canada in a warmer climate. *Climate Dynamics*, 54(3), 2493-2509.

Parameswaran, V. (1978). Adfreeze strength of frozen sand to model piles. *Canadian geotechnical journal*, 15(4), 494-500.

Parameswaran, V. (1979). Creep of model piles in frozen soil. *Canadian geotechnical journal*, 16(1), 69-77.

Paul, Jason, Baltzer, Jennifer L., Kokelj, Steve V., (2020), "Near-surface permafrost ground ice characteristics and ecological and physical drivers of transient layer ice content in discontinuous permafrost near Yellowknife, NT", <https://doi.org/10.5683/SP2/LX5IJN>, Scholars Portal Dataverse.

Pavlov A. V. (1975). Soil Heat Exchange with Atmosphere at Northern and Middle Latitudes. Third International Conference on Permafrost, Edmonton. Yakutsk (In Russian).

Pelletier, J., Broxton, P., Hazenberg, P., Zeng, X., Troch, P., Niu, G., Williams, Z., Brunke, M., and Gochis, D. (2016). Global 1-km gridded thickness of soil, regolith, and sedimentary deposit layers. *ORNL DAAC*.

Pelletier, J., Broxton, P., Hazenberg, P., Zeng, X., Troch, P., Niu, G., Williams, Z., Brunke, M., and Gochis, D. (2016). Global 1-km gridded thickness of soil, regolith, and sedimentary deposit layers. *ORNL DAAC*.

Perko, H. A. (2009). Helical piles: a practical guide to design and installation. John Wiley & Sons.

Perreault, P., and Shur, Y. (2016). Seasonal thermal insulation to mitigate climate change impacts on foundations in permafrost regions. *Cold regions science and technology*, 132, 7-18.

Pihlainen, J. A. (1959). Pile construction in permafrost. *Journal of the Soil Mechanics and Foundations Division*, 85(6), 75-95.

Pithan, F., and Mauritsen, T. (2014). Arctic amplification dominated by temperature feedbacks in contemporary climate models. *Nature geoscience*, 7(3), 181-184.

Plotnikov, A. A., and Makarov, V. I. (2017). Methods of cooling the foundations of buildings constructed according to the principle of maintaining the soil in a permafrost state (town of Mirnyi). *Soil Mechanics and Foundation Engineering*, 54(5), 341-348.

Porkhaev, G.V. (1970). Thermal Interaction of Buildings and Perennially Frozen Ground. Nauka Publishing House, Moscow (In Russian).

Prein, A. F., Gobiet, A., Suklitsch, M., Truhetz, H., Awan, N. K., Keuler, K., and Georgievski, G. (2013). Added value of convection permitting seasonal simulations. *Climate Dynamics*, 41(9-10), 2655-2677.

Prein, A. F., Holland, G. J., Rasmussen, R. M., Done, J., Ikeda, K., Clark, M. P., and Liu, C. H. (2013). Importance of regional climate model grid spacing for the simulation of heavy precipitation in the Colorado headwaters. *Journal of climate*, 26(13), 4848-4857.

Prein, A. F., Langhans, W., Fosser, G., Ferrone, A., Ban, N., Goergen, K., ... and Leung, R. (2015). A review on regional convection-permitting climate modeling: Demonstrations, prospects, and challenges. *Reviews of geophysics*, 53(2), 323-361.

Ran, Y., Li, X., and Cheng, G. (2018). Climate warming over the past half century has led to thermal degradation of permafrost on the Qinghai–Tibet Plateau. *The Cryosphere*, 12(2), 595-608.

Riahi, K., Rao, S., Krey, V., Cho, C., Chirkov, V., Fischer, G., Kindermann, G., Nakicenovic, N., and Rafaj, P. (2011). RCP 8.5—A scenario of comparatively high greenhouse gas emissions. *Climatic change*, 109(1), 33-57.

Rummukainen, M. (2010). State-of-the-art with regional climate models. *Wiley Interdisciplinary Reviews: Climate Change*, 1(1), 82-96.

Sanger, F. J. (1969). *Foundations of structures in cold regions*. US Army Materiel Command, Terrestrial Sciences Center, Cold Regions Research

Serreze, M. C., and Barry, R. G. (2011). Processes and impacts of Arctic amplification: A research synthesis. *Global and planetary change*, 77(1-2), 85-96.

Shiklomanov, N. I., Streletskiy, D. A., Grebenets, V. I., and Suter, L. (2017). Conquering the permafrost: urban infrastructure development in Norilsk, Russia. *Polar Geography*, 40(4), 273-290.

Shiklomanov, N. I., Streletskiy, D. A., Swales, T. B., and Kokorev, V. A. (2017). Climate change and stability of urban infrastructure in Russian permafrost regions: prognostic assessment based on GCM climate projections. *Geographical review*, 107(1), 125-142.

Shur, Y., and Goering, D. J. (2009). Climate change and foundations of buildings in permafrost regions. In *Permafrost soils* (pp. 251-260). Springer, Berlin, Heidelberg.

Shur, Y., Nidowicz, B., Kamenskiy, R.M., Slavin-Borovski, V.B., (2004). Permafrost thawing

Smith, S., Riseborough, D., Ednie, M., and Chartrand, J. (2013). A map and summary database of permafrost temperatures in Nunavut. *Canada, Geological Survey of Canada, Open File*, 7393.

SNiP II-B.6-66. Bases and Foundations on Permafrost [in Russian], Stroiizdat (1966).

SP 25.13330.2012, (2012). Basements and Foundations on Permafrost. Ministry of Regional Development of the Russian Federation, Moscow.

Streletskiy, D. A., Suter, L. J., Shiklomanov, N. I., Porfiriev, B. N., and Eliseev, D. O. (2019). Assessment of climate change impacts on buildings, structures and infrastructure in the Russian regions on permafrost. *Environmental Research Letters*, 14(2), 025003.

Streletskiy, D. A., Shiklomanov, N. I., and Nelson, F. E. (2012). Permafrost, infrastructure, and climate change: a GIS-based landscape approach to geotechnical modeling. *Arctic, Antarctic, and Alpine Research*, 44(3), 368-380.

Stuecker, M. F., Bitz, C. M., Armour, K. C., Proistosescu, C., Kang, S. M., Xie, S.-P., Kim, D., McGregor, S., Zhang, W., and Zhao, S. (2018). Polar amplification dominated by local forcing and feedbacks. *Nature Climate Change*, 8(12), 1076-1081.

Sundqvist, H., Berge, E., and Kristjánsson, J. E. (1989). Condensation and cloud parameterization studies with a mesoscale numerical weather prediction model. *Monthly weather review*, 117(8), 1641-1657.

Suter, L., Streletskiy, D., and Shiklomanov, N. (2019). Assessment of the cost of climate change impacts on critical infrastructure in the circumpolar Arctic. *Polar Geography*, 42(4), 267-286.

Teufel, B., and Sushama, L. (2021). High-resolution modelling of climatic hazards relevant for the northern transportation sector. (Submitted).

Teufel, B., Sushama, L., Huziy, O., Diro, G. T., Jeong, D. I., Winger, K., ... and Nguyen, V. T. V. (2019). Investigation of the mechanisms leading to the 2017 Montreal flood. *Climate Dynamics*, 52(7), 4193-4206.

Thornton, P., Thornton, M., Mayer, B., Wei, Y., Devarakonda, R., Vose, R., and Cook, R. (2016). Daymet: daily surface weather data on a 1-km grid for North America, version 3. ORNL DAAC, Oak Ridge, Tennessee, USA. In *USDA-NASS, 2019. 2017 Census of Agriculture, Summary and State Data, Geographic Area Series, Part 51, AC-17-A-51*.

Wagner, A. M. (2014). Review of thermosyphon applications.

Weaver, J., and Morgenstern, N. (1981). Pile design in permafrost. *Canadian geotechnical journal*, 18(3), 357-370.

Yu, Q., Ji, Y., Zhang, Z., Wen, Z., and Feng, C. (2016). Design and research of high voltage transmission lines on the Qinghai–Tibet Plateau—A Special Issue on the Permafrost Power Lines.

Zadra, A., McTaggart-Cowan, R., and Roch, M. (2012). Recent changes to the orographic blocking parametrization.

Zarling, J. and Yarmak, E. (2007). Refrigerated Foundations. In: E. Clarke, ed., *Permafrost Foundation: State of the Practice*. American Society of Civil Engineers, p.73.

Zhao, Y., and Sushama, L. (2020). Aircraft Takeoff Performance in a Changing Climate for Canadian Airports. *Atmosphere*, 11(4), 418.